On Optimal Energy-Efficient Transmission Scheduling for Remote State Estimation

Bowen Sun, *Member, IEEE*, Xianghui Cao, *Senior Member, IEEE*, Wei Xing Zheng, *Fellow, IEEE* and Yu Cheng, *Fellow, IEEE*

***Abstract*—The problem of sensor scheduling under resource constraints in remote state estimation systems has been extensively studied in the past. While many sophisticated scheduling policies have been proposed, practically most wireless sensors operate in the simple strictly periodic pattern for sampling and packet transmission. In this paper, from an energy-efficiency perspective that jointly considers remote estimation accuracy and sensor energy consumption, we provide a rigorous explanation that a strictly periodic sensor scheduling policy can arbitrarily approximate the optimal energy-efficient policy. From this foundation, we explicitly characterize the optimal periodic scheduling, underscoring that: 1) There exists a unique strictly periodic scheduling policy which is optimal among all periodic policies; 2) An exact expression of the optimal period of the strictly periodic policy is derived, which is solely dependent on the packet dropout rate of the communication channel and the spectral radius of the system matrix. Numerical results validate our theoretical findings.**

***Index Terms*—Sensor scheduling, energy efficiency, state estimation, optimization, periodic scheduling.**

I. Introduction

With the advancement of industrial manufacturing technology, remote state estimation systems have been developed to achieve wireless connectivity, intelligence, and convenient deployment capabilities, which in turn has spurred the mass production of small wireless sensors. These sensors are used for data collection and information transmission, facilitating monitoring, feedback control, and decision making [1]. Given the limited energy resources of the sensor node, transmission scheduling of wireless sensors needs to be properly designed to guarantee remote estimation performance [2]. Within this context, the periodic scheduling policy for sensors is widely utilized [3].

Since data packet transmission incurs energy consumption, enhancing the system performance often leads to higher energy usage; hence, it is generally improbable to achieve both performance maximization and energy minimization simultaneously. Regarding the management of these conflicting objectives, most research studies still prioritize one goal as the aim of the optimization problem, while treating the other as a constraint. According to [4], the optimal solution for transmission scheduling under hard energy constraints necessarily entails the complete utilization of all available energy. Using all the available energy results in a waste of resources, and additional transmissions do not necessarily yield a linear performance gain when the estimation error is close to convergence [5]. This undermines our primary objective of reducing energy consumption, except when a smaller energy constraint is predetermined, which is typically dependent on expert experience.

If energy constraints are incorporated and weighted into the objective function for optimization, the following limitations can be observed: firstly, the physical significance of such weighting is not yet clear, and secondly, the result of the scheduling is highly contingent upon the selected weight values, which does not allow for a precise definition of whether the optimal system performance has been achieved or the minimum energy consumption has been attained. It is noticeable that the literature utilizing this method can only assert that it results in relatively lower energy consumption, without formally defining the relationship between energy consumption and system performance. Thus, we aim to discover a method that not only clearly achieves our energy-saving goals but also ensures that the energy efficiency is optimized. To this end, we introduce the concept of "energy efficiency".

We leverage the concept of energy efficiency to the ratio of system performance to consumed energy. It is an established and recognized metric within the network communication domain [6]. Energy efficiency can help improve overall system performance while reducing energy consumption. Therefore, in this paper, we target the theoretical optimal energy efficiency of system performance and discuss the conditions and theoretical solutions to obtain the optimal energy efficiency.

This paper considers the optimal sensor scheduling problem within a remote state estimation system over a random Bernoulli packet-dropping channel. Our objective is to realize a sensor scheduling policy that maximizes the energy efficiency. Unlike previous studies that emphasized sensor scheduling with energy constraints to improve system performance, our work focuses on transmission scheduling policies designed to maximize energy efficiency, which we believe is innovative in the context of remote state estimation systems. We begin by proving that periodic scheduling can arbitrarily approximate any schedule over an infinite time horizon when the objective function is the optimal energy efficiency, a

Manuscript received 30 September 2024; revised 16 January 2025; accepted 28 February 2025. This work was supported in part by the Frontier Technologies R&D Program of Jiangsu Province under Grant BF2024065, and in part by the Shenzhen Science and Technology Program under Grant JCYJ20230807114609019. The work of Yu Cheng was supported in part by the National Science Foundation (NSF) under Grant CNS-2008092.

B. Sun and X. Cao are with the School of Automation, Southeast University, Nanjing 210096, China (e-mail: bwsun@seu.edu.cn, xhcao@seu.edu.cn).

W. X. Zheng is with the School of Computer, Data and Mathematical Sciences, Western Sydney University, Sydney, NSW 2751, Australia (e-mail: w.zheng@westernsydney.edu.au).

Y. Cheng is with the Department of Electrical and Computer Engineering, Illinois Institute of Technology, Chicago, IL 60616 USA (e-mail: cheng@iit.edu).

conclusion that simplifies the problem and makes proposing an offline scheduling policy possible. Subsequently, we provide a rigorous proof that a strictly periodic schedule represents the unique and optimal periodic policy solution for achieving the maximum energy efficiency. This foundation enables us to elaborate on the details of periodic scheduling strategies. Building upon the strictly periodic scheduling policy, we reformulate the problem and derive explicit solutions for the periodic schedule duration, accommodating variations in system parameters and packet drop rates. Consequently, we present a comprehensive offline sensor scheduling framework based on optimizing energy efficiency. The main contributions of this paper are summarized as follows.

- We demonstrate that, with the optimization goal being energy efficiency, a periodic scheduling scheme can arbitrarily approximate any given schedule over an infinite time horizon.
- We derive that the optimal periodic schedule for maximizing energy efficiency is strictly periodic and that such a schedule exists uniquely.
- We theoretically provide an optimal strict period length, and our simulations reveal that the system performance is a concave function with respect to the period length.

The remainder of this paper is organized as follows. Section II shows the related works. Section III describes the system model of remote state estimation and formulates the problem of energy efficiency optimization. Section IV presents some theoretical analysis and shows the optimality of the scheduling policy. Section V provides the optimal period length. The numerical results are presented in Section VI. Finally, Section VII offers the conclusion.

Notations: Sets and matrices are represented by calligraphic uppercase and regular uppercase letters, respectively, such as $\mathcal{X}$ for sets and X for matrices. The n-dimensional Euclidean space is denoted by $\mathbb{R}^n$. For a matrix X, the trace, transpose, and spectral radius are denoted by $\mathrm{Tr}(X)$, X', and $\rho(X)$, respectively. The expectation and probability of a random variable are represented respectively by $\mathbb{E}[\cdot]$ and $\Pr(\cdot)$.

II. Related Work

Amidst the evolution of networks, energy efficiency constituted a fundamental prerequisite, characterized by an increase in system performance per unit of energy consumed [7], [8]. In [9], the energy efficiency of cloud computing services, whose data centers were distributed and interconnected through cloud networks was optimized. In [10], the transmission quality of distributed sensor nodes was characterized by the energy efficiency indicator. While the energy efficiency was commonly used in the field of network communications to balance network system performance and energy consumption, its application in the areas of control and estimation remained limited.

Building on the interplay between energy consumption and system performance, researchers investigated various scheduling methodologies. Typically, these methods were divided into offline and online cases. However, in this paper, we focus more on the impact of constraints on our optimization objectives. Therefore, we classify the problem into two common approaches: one where hard constraints are present and the other where constraints are weighted into the optimization objectives in the form of soft constraints. For the transmission scheduling with hard energy constraints, a similar "periodic" scheduling structure has been observed in throughput optimization problems [11]–[15]. In [11], an optimal sensor scheduling policy based on high-low energy consumptions was proposed to transmit data packets. It provided the first proof that transmission scheduling under energy constraints tends to periodic distribution. This is the basis for further work in [12] which explained that under energy constraints, the difference in interval lengths between transmission to the next transmission in the optimal periodic scheduling policy is limited to 0 or 1. In [13], [14], the periodic scheduling policy was extended from a finite time horizon to an infinite time horizon, proving that under the premise of energy hard constraints, the periodic scheduling policy can infinitely approximate any feasible policy.

The need to address sensor scheduling in the context of energy constraints was spurred the development of various modeling frameworks. In [16], the open-loop estimation system was extended to closed-loop control systems, and a heuristic algorithm was designed to study the suboptimal control period intervals which tend to distribute uniformly. In [17], a suboptimal, lightweight scheduling method was introduced to tackle the challenge arising from invalid Gaussian assumptions in the estimator due to stochastic event-triggering mechanisms. Additionally, research on optimal scheduling policies was presented in [18] for energy-constrained environments involving multiple sensors, and for multi-hop sensor networks in [19]. Learning-based online optimization methods, such as Markov Decision Processes (MDP) and multi-agent reinforcement learning, were also employed to formulate optimal policies in [20] and [21].

For the transmission scheduling with energy weighted, similar problems were studied in [22]–[25]. In [22], an event-based hybrid integer linear programming algorithm was proposed to optimize the scheduling of weighted non-preemptive resources under energy constraints. The work in [23] investigated how to optimally schedule sensor transmissions with reduced energy consumption using an MDP framework. In [25], the loss in system performance caused by transmission power was included in the optimization objective. Further, incorporating energy as hard constraints and as soft constraints into the optimization problem was compared in terms of optimality in [24]. Additionally, there were several feasible scheduling methods, such as start scheduling and probability-based scheduling, which involve incorporating scheduling variables as random variables or using probabilistic constraints to achieve the scheduling objectives. In [26]–[28], a series of transmission scheduling methods based on probabilistic constraints and probabilistic variable distributions were proposed. These methods leverage Bayesian learning to capture the uncertainty in the transmission process and implement a range of near-optimal scheduling approaches.

Existing researches on system performance scheduling were made several progress in addressing the trade-offs between performance and energy consumption. However, these meth-

ods exhibited certain limitations. Hard constraints often led to solutions that exhaust all available energy, which may be suboptimal in scenarios where energy efficiency was prioritized over pure performance. Learning-based methods introduced additional complexity, requiring extensive training or computational resources. Furthermore, most studies focused on maximizing performance under predefined energy constraints, rather than directly optimizing energy efficiency as a primary objective.

III. System Setup and Problem Formulation

In this paper, we discuss a remote estimation problem, where the estimator generates state estimates based on the received information from the sensor. The architecture of the system is depicted in Fig. 1, and the primary components are detailed in the following subsections.

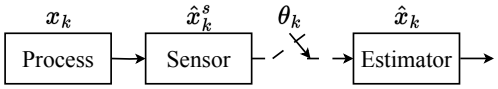

Fig. 1: System architecture.

A. Process model

We consider the following discrete linear time-invariant (LTI) process,

$$x_{k+1} = Ax_k + w_k, \tag{1}$$
$$y_k = Cx_k + v_k, \tag{2}$$

where $x_k \in \mathbb{R}^n$ is the state of the dynamic process, $y_k \in \mathbb{R}^n$ is the corresponding sensor measurement, and w_k and v_k are mutually independent zero-mean Gaussian noises with covariances Q and R, respectively. We assume that the pair $(A, \sqrt{Q})$ is stabilizable and the pair (A, C) is observable.

We assume that the sensor has sufficient storage and computational capacity, which can effectively reduce the impact of packet dropout during unreliable wireless communication [29]. Upon obtaining the measurement y_k, the sensor executes a localized Kalman filter (**KF**) to calculate the minimum mean square error (MMSE) estimate, denoted as $\hat{x}_k^s$ and its corresponding error covariance P_k^s [30], i.e.,

$$(\hat{x}_k^s, P_k^s) = \mathbf{KF}\left(\hat{x}_{k-1}^s, P_{k-1}^s, y_k\right), \tag{3}$$

here, the operator **KF** satisfies:

$$\begin{aligned}
\hat{x}_{k,k-1}^s &= A\hat{x}_{k-1}^s, \\
P_{k,k-1}^s &= AP_{k-1}A' + Q, \\
K_k^s &= P_{k,k-1}^s C'(CP_{k,k-1}^s C' + \Sigma_v)^{-1}, \\
\hat{x}_k^s &= \hat{x}_{k,k-1}^s + K_k^s(y_k - C\hat{x}_{k,k-1}^s), \\
P_k^s &= (I - K_k^s C)P_{k,k-1}^s,
\end{aligned}$$

where $\hat{x}_{k,k-1}^s$ and $P_{k,k-1}^s$ are the *a priori* estimate and corresponding estimation error covariance, respectively. $\hat{x}_k^s$ and P_k^s are the *a posteriori* estimate and corresponding estimation error covariance, respectively. K_k^s is the filter gain, and I is the identity matrix. The Kalman filter operates recursively, starting with $\hat{x}_0^s = 0$ and $P_0^s = \Xi$. Since we assume that the initial error covariance matrix $\Xi > 0$, and $(A, \sqrt{Q})$ is stabilizable and (A, C) is observable, according to [31], P_k^s converges exponentially to a steady state $\bar{P}$. Without loss of generality, we assume that the local Kalman filter operates in the steady state, i.e., $P_k^s = \bar{P}, \forall k \geq 1$.

B. Communication and energy model

The sensor transmits its state estimates to the remote estimator via an unreliable wireless channel. We model the packet-dropping state of channel by a Bernoulli random process $\mu_k = \{0, 1\}$, where $p = \Pr(\mu_k = 1)$ denotes the probability (with $0 < p \leq 1$) of successful packet transmission[1]. The binary variable θ_k determines whether transmission occurs at time k, where $\theta_k = 1$ indicates transmission and $\theta_k = 0$, otherwise.

The energy expended by the sensor node during operation can be abstractly divided into two distinct parts [32]: the first part corresponds to the energy consumed by the processing circuitry, E_{proc}, which is present regardless of data transmission, including the energy consumed for computational tasks, such as executing a local Kalman filter or other estimation algorithms; the second part accounts for the energy consumption of the power amplifier in the transmitter, E_{tx}, whose energy consumption primarily hinges on the transmission energy per bit, E_{bit}, and fluctuates with the size of the data packet. Given that the data packet size is consistently set at b bits per transmission, the energy model for the sensor's transmission is outlined as follows:

$$E_{k,\text{sensor}} = \begin{cases} E_{\text{tx}} + E_{\text{proc}}, & \text{when } \theta_k = 1, \\ E_{\text{proc}}, & \text{otherwise.} \end{cases} \tag{4}$$

Generally, the energy consumption by E_{proc} is negligible when compared to the energy used for transmission [33], and given that E_{proc} remains a constant at all times, it is also a constant in the overarching optimization problem. Therefore, we propose to omit E_{proc} from our considerations.

C. Remote state estimation model

The remote estimator receives transmitted packets based on the channel realization, i.e., $\xi_k = \mu_k\theta_k$. The estimation error covariance P_k evolves as:

$$P_k = \begin{cases} \bar{P}, & \text{if } \xi_k = 1, \\ h\left(P_{k-1}\right), & \text{otherwise,} \end{cases} \tag{5}$$

where the Lyapunov operator $h(\cdot)$ is defined as $h(X) = AXA' + Q$. According to [34, Lemma 3.1], the operator $h^t(X)$ increases monotonically with respect to t, e.g., if $t_1 \leq t_2$ for $t_1, t_2 \in \mathbb{N}$, then $h^{t_1}(X) \leq h^{t_2}(X)$.

Define the time elapsed since the last packet received by the sensor at the current time step k, i.e.,

$$\tau_k = \min_t\{0 \leq t \leq k : \xi_{k-t} = 1\}. \tag{6}$$

[1]The proposed scheme assumes a Bernoulli random packet-dropping channel. For more complex channels, such as Rayleigh fading or time-varying channels, additional considerations would be required to adapt the method, which is left for the future work.

Thus, the estimation error covariance of the remote estimator can be compactly written as:

$$P_k = h^{\tau_k}(\bar{P}). \tag{7}$$

D. Problem of interest

We focus on the sensor's decisions $\theta_k \in \{0, 1\}$ whether the sensor is scheduled to transmit a data packet at each time k. We denote by $\boldsymbol{\theta} = \{\theta_k\}_k^\infty$ an admissible scheduling policy and by Θ the causal set of all admissible policies, respectively.

For a given $\boldsymbol{\theta}$, we define the average estimation error covariance of the remote estimator as:

$$J_e(\boldsymbol{\theta}) = \lim_{N\to\infty} \frac{1}{N} \sum_{k=0}^{N-1} \mathrm{Tr}(P_k), \tag{8}$$

and meanwhile, the average transmission energy of the sensor is denoted by:

$$J_r(\boldsymbol{\theta}) = \lim_{N\to\infty} \frac{1}{N} \sum_{k=0}^{N-1} \theta_k \cdot E_{\mathrm{tx}}, \tag{9}$$

where, E_{tx} is assigned a unit value of 1 for the purpose of subsequent analysis.

Our objective is to maximize the energy efficiency of the system, reflecting our focus on sensor-energy savings while taking system performance into account. In other words, our goal is to maximize the ratio of system performance to energy consumption. The system performance can be quantified by the average estimation error covariance; the smaller $J_e(\boldsymbol{\theta})$, the better the system performance. Therefore, we define the system performance as the reciprocal of the average error covariance $J_e(\boldsymbol{\theta})$ and aim to maximize the ratio of $1/J_e(\boldsymbol{\theta})$ to $J_r(\boldsymbol{\theta})$. Clearly, this problem could be further simplified. We define the objective function as:

$$J(\boldsymbol{\theta}) = J_e(\boldsymbol{\theta}) \cdot J_r(\boldsymbol{\theta}). \tag{10}$$

Subsequently, we obtain an equivalent formulation for maximizing the system energy efficiency as Problem 1:

Problem 1.

$$\min_{\boldsymbol{\theta}\in\Theta} \quad J(\boldsymbol{\theta}). \tag{11}$$

To directly capture the trade-off between system performance and energy consumption, we design $J(\boldsymbol{\theta})$, which avoids the subjectivity of weight selection in weighted sum methods and ensures that optimization focuses on energy efficiency. Our focus has increasingly shifted towards the system improvements brought about by each unit of energy, rather than solely achieving scheduling objectives without regard to energy consumption. Obviously, $J_r(\boldsymbol{\theta})$ is energy-dependent—the larger J_r, the higher the energy consumption of the sensor, and correspondingly, $J_e(\boldsymbol{\theta})$ should be smaller. In some cases, we prefer not to expend excessive energy to maintain system performance. Further, we normalize energy consumption per transmission. Many researchers model energy consumption as a constraining factor, ensuring that optimal policies are derived within the bounds of a maximum energy limit [11], [12]. However, this approach may lead to an insufficient distribution of energy at critical points due to the inherently discrete nature of integer optimization problems. This motivates us to construct the energy efficiency function as the optimization objective. It is similar to some kind of diminishing returns, due to each local estimate being stochastically equivalent and statistically independent. As transmission frequency increases, the additional information gained decreases. Marginal performance gain approaches zero, but energy consumption continues to increase linearly. This motivates us to construct the energy efficiency function as the optimization objective.

IV. Optimality of Strictly Periodic Scehduling

The solution space of Problem 1 is boundless, rendering the optimal solution challenging to attain. Nevertheless, a periodic scheduling policy has the ability to closely approximate any other policies. Hence, our focus will be on the investigation of periodic scheduling policies.

A. Periodic scheduling policy

The scheduling problem involves exploring a giant decision space (2^N decisions for a finite horizon N), making it computationally intractable. We give the following lemma to show that the problem is NP-hard.

Lemma 1. *Problem 1 is NP-hard.*

Proof. We prove the NP-hardness of the problem by reduction from the *Subset Sum* problem (SP13 problem in [35]): give a finite set $\mathcal{R} = r_1, r_2, \ldots, r_N$, size $s(r_n) \in \mathbb{Z}^+$, $\forall r_n \in \mathcal{R}, n = 1, 2, \ldots, N$, and positive integers B. The question is whether there is a subset $\mathcal{R}' \subseteq \mathcal{R}$ such that the sum of the sizes of the elements in $\mathcal{R}'$ is exactly B satisfying $\sum_{r_n\in\mathcal{R}'} r_n = B$.

For ease of exposition, we abuse the previously defined notation and omit the time index k. For the reduction, we first create a sequence of N decision steps, indexed by $n = 1, 2, \ldots, N$. At the n-th step, the sensor chooses either $\theta = 0$ or $\theta = 1$, i.e., $\theta = 1$ will be interpreted as "select the integer r_n"; $\theta = 0$ will be interpreted as "do not select r_n". After the sense has made the choice, the holding time τ either resets to 0 with probability p (if $\theta = 1$) or else continues incrementing $\tau \leftarrow \tau + 1$. The cost at each time step is given by $\theta \mathrm{Tr}\left(h^\tau(\bar{P})\right)$. We will ensure that there is a large bonus only if $\sum_{r_n\in\mathcal{R}'} r_n = B$.

We can keep track of the partial sums in a straightforward way: at the n-th step, choosing $\theta = 1$ indicates we are "adding r_n". To verify that the sum is exactly B, we embed a check at the end of the N steps: if the sum equals B, then we transition with probability 1 to a special "bonus" regime. In the bonus regime, we let τ reset to 1 and allow enough time steps such that $\theta \mathrm{Tr}\left(h^\tau(\bar{P})\right)$ from that bonus regime alone exceeds $\bar{B}$, provided that the policy has indeed formed the sum B. If the sum is not B, then that reset never happens, keeping the total below $\bar{B}$.

Then, the mapping from the *Subset Sum* problem to our optimal solution of Problem 1 is straightforward: we introduce N decision steps and an end-of-horizon check, all definable in time polynomial. As SP13 is NP-hard, Problem 1 is also NP-hard, which proves the theorem. □

Next, in practical applications, it is worthwhile to propose a simple and effective scheduling policy that is less resource-consuming. To address this challenge, we focus on periodic scheduling policies. These policies significantly reduce the decision space while preserving the ability to closely approximate optimal solutions, thus providing a computationally efficient framework for analysis.

The periodic scheduling policy $\boldsymbol{\theta}_p$, represents a scheduling policy that repeats itself with a fixed period. The subscript p indicates periodicity. It is defined as follows:

$$\boldsymbol{\theta}_p = (\theta_i : i = k \bmod T), \tag{12}$$

where $\theta_0 = 1$ and $\theta_i = 0$ or 1, $\forall i \in \{1, 2, \ldots, T-1\}$. This means that the transmission decision at time k depends on the remainder when k is divided by the period T. The period $T \in \mathbb{Z}_+$ is finite. Denote by Θ_p the set of all admissible periodic policies.

For a given periodic schedule $\boldsymbol{\theta}_p$, the scheduling period is indicated by T, and the number of transmissions in the period is denoted by m, where $m = \sum_i^T \theta_i$ and $m \leq T$. Let $\mathcal{T} = (t_1, t_2, \ldots, t_m)$ indicate the time interval between each sensor's decision for transmission, i.e., $\sum_{i=1}^m t_m = T$. Then each policy $\boldsymbol{\theta}_p$ can be defined precisely as a function of t:

$$\boldsymbol{\theta}_p(\mathcal{T}) = (1, \underbrace{0, \ldots, 0}_{t_1-1 \text{ times}}, 1, \underbrace{0, \ldots, 0}_{t_2-1 \text{ times}}, \ldots, 1, \underbrace{0, \ldots, 0}_{t_m-1 \text{ times}}), \tag{13}$$

where $t_i - 1$ is denoted by the number of 0's after the i-th 1 in $\boldsymbol{\theta}_p$. For example, given $\mathcal{T} = (1, 2, 3)$, we have $\boldsymbol{\theta}_p(\mathcal{T}) = (1, 1, 0, 1, 0, 0)$.

After defining the periodic scheduling policy, we need to explore its availability. The following theorem shows that for any given arbitrary infinite time horizon schedule, there exists a periodic schedule that can approximate it arbitrarily closely. Therefore, our optimization objective can also be approximated through periodic scheduling in terms of limits.

Theorem 1. *For any feasible schedule $\boldsymbol{\theta} \in \Theta$, and any $\varepsilon > 0$, there exists a periodic schedule $\boldsymbol{\theta}_p$, such that the infinite horizon objective $J(\boldsymbol{\theta})$ of $\boldsymbol{\theta}$ is approximated by $\boldsymbol{\theta}_p$ with the error bound $|J(\boldsymbol{\theta}) - J(\boldsymbol{\theta}_p)| < \varepsilon$.*

Proof. We divide the main proof into three steps. To begin with, we clarify that the initial error covariance poses no impact on our intended objective function. Next, we introduce the concept of limits and prove that there exists a scheduling policy with a certain K such that for any time $k > K$, our error requirement ε is satisfied. Finally, by applying mathematical induction, we show that the introduction of a periodic strategy can also meet these requirements. Refer to Appendix A for detailed steps. □

Such an approach allows us to only consider a relaxed and simple periodic scheduling policy so as to arbitrarily approximate the performance of the optimal solution, rather than finding the optimal solution among all feasible schedules. Consequently, we consider the following optimization problem with periodic scheduling policy:

Problem 2.

$$\min_{\boldsymbol{\theta}_p \in \Theta_p} \quad J(\boldsymbol{\theta}_p). \tag{14}$$

B. Problem reformulation

Notice that a coupling is formed between the error covariance and energy consumption in Problem 2, which causes difficulties in solving it. Thus, we first try to reformulate Problem 2 to avoid the coupling relationship. Intuitively, we could express the subject function of Problem 1 as:

$$\begin{aligned} J(\boldsymbol{\theta}_p) &= \lim_{N\to\infty} \frac{1}{N} \sum_{k=0}^{N-1} \theta_k \times \lim_{N\to\infty} \frac{1}{N} \sum_{k=0}^{N-1} \mathrm{Tr}(P_k) \\ &\overset{\text{(a)}}{=} \frac{m}{T} \lim_{N\to\infty} \frac{1}{N} \sum_{k=0}^{N-1} \mathrm{Tr}(P_k) = \frac{m}{T} J_e(\boldsymbol{\theta}_p), \end{aligned} \tag{15}$$

where (a) holds by the Markov law of large numbers. Thus, we can derive the following problem based on the periodic policy.

Problem 3.

$$\min_{\boldsymbol{\theta}_p \in \Theta_p} \quad \frac{m}{T} J_e(\boldsymbol{\theta}_p). \tag{16}$$

C. Optimal periodic scheduling policy

In this subsection, we theoretically examine the explicit properties of the optimal periodic scheduling policy. To this end, we require the following result from [12].

Lemma 2 ([12, Lemma 2])**.** *For a fixed $\frac{m}{T}$, the optimal periodic policy to minimize $J_e(\boldsymbol{\theta}_p)$ satisfies:*

$$\left| \sum_{i=d_1}^{d_1+u} t_i - \sum_{i=d_2}^{d_2+u} t_i \right| = 0 \text{ or } 1, \tag{17}$$

for any $d_1, d_2 \in \{1, 2, \ldots, m\}$ and $u \in \{0, 1, \ldots, m-1\}$.

The next lemma describes that an optimal periodic scheduling policy $\boldsymbol{\theta}_p^*$ always exists and that its scheduling period is bounded.

Lemma 3 (Existence of the optimal periodic policy)**.** *The optimal periodic scheduling policy $\boldsymbol{\theta}_p^*$ for Problem 2 always exists, and its scheduling period is finite.*

Proof. First, according to Lemma 2, for a fixed $\frac{m}{T}$, the optimal value with respect to minimizing $\frac{m}{T} J_e(\boldsymbol{\theta}_p)$ is also constrained within a specific range. Meanwhile, as $\frac{m}{T}$ increases, the transmission interval between packets decreases, which means that the average τ, i.e., $\lfloor \frac{m}{T} \rfloor$, for each transmission also decreases, thereby reducing the average error covariance $J_e(\boldsymbol{\theta}_p)$. Therefore, the optimal periodic policy to minimize $\frac{m}{T} J_e(\boldsymbol{\theta}_p)$ will be selected based on the variations in the value of $\frac{m}{T}$, employing a method akin to that described in Lemma 2. That is, a finite range always exists within which the optimal periodic policy to minimize $\frac{m}{T} J_e(\boldsymbol{\theta}_p)$ can be found. □

Thanks to the stricter restrictions of Lemma 3, we have the following elegant result on the optimal policy for Problem 3.

Theorem 2. *The optimal policy is strictly periodic, i.e.,*

$$\boldsymbol{\theta}_p^* = \boldsymbol{\theta}_{sp}(T) = (1, \underbrace{0, 0, \cdots}_{T-1 \text{ times}}), \tag{18}$$

where the period of the strictly periodic policy is T.

Proof. The detailed proof can be seen in Appendix B. □

Naturally, we can immediately derive the following corollary to show the optimal policy choice in the fixed energy efficiency case, i.e., m and T are both constants.

Corollary 1. *If m and T are both fixed, the period of optimal energy-efficient policy is $\lfloor \frac{m}{T} \rfloor + 1$.*

Proof. The proof is included in Appendix B, thus not repeated here. □

D. Stability condition

Next, it is essential to evaluate the stability condition of the objective function $J(\boldsymbol{\theta}_{sp})$. The relevance of our results is contingent upon them falling within the convergence limits. In other words, the stability condition we propose refers to the convergence of $J(\boldsymbol{\theta}_{sp})$, with the convergence value being bounded and reaching a deterministic value. Additionally, evaluating the stability condition helps narrow down the practical range of our objective function. Following Theorem 2, $J(\boldsymbol{\theta}_{sp})$ can be reformulated as $\frac{1}{T}J_e(\boldsymbol{\theta}_{sp})$. Therefore, according to [12, Theorem 4], we obtain the following lemma,

Lemma 4. *$J(\boldsymbol{\theta}_{sp})$ is stable if and only if*

$$\rho^{2T}(A)(1-p) < 1. \tag{19}$$

We demand that the packet dropout rate and the system dynamics satisfy the above (19) to ensure that $J(\boldsymbol{\theta})$ does not diverge as $T \to \infty$, guaranteeing the feasibility of Problem 3. This stability condition also ensures that the proposed energy-efficient scheduling policy is meaningful, as unstable objectives would lead to impractical solutions [36]. Therefore, our subsequent discussions will be based on (19) in Lemma 4.

Remark 1. *In our work, the stability condition ensures that system performance remains acceptable, thereby preventing scenarios where extremely low energy consumption (i.e., a very long scheduling period) leads to high energy efficiency but poor performance.*

V. The Optimal Period Length

In the preceding section, we have demonstrated that the scheduling policy we propose exhibits strict periodicity. We have also provided the stability conditions necessary for the existence of the optimal periodic policy. Consequently, in this section, we will consider only the optimal periodic policy under stable conditions. We will first reformulate the model before attempting to determine the exact optimal period length, thereby solving this problem from a numerical perspective.

As shown in Fig. 2, Problem 3 is reformulated as Problem 4.

Problem 4.

$$\min_{\boldsymbol{\theta}_{sp} \in \Theta_{sp}} \quad J(T) \triangleq \frac{1}{T} J_e(\boldsymbol{\theta}_{sp}), \tag{20}$$

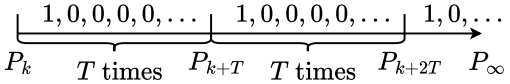

Fig. 2: Optimal periodic transmission policy.

where Θ_{sp} is denoted by the set of all admissible strictly periodic policies. The policy $\boldsymbol{\theta}_{sp}$ corresponds one-to-one with the period T, allowing the exchange between them in the following analysis, i.e., $J(\boldsymbol{\theta}_{sp}) \triangleq J(T)$.

Before proceeding with further analysis, it is necessary to establish that the optimal period T is unique.

Lemma 5 (Uniqueness of the optimal periodic policy)**.** *For Problem 4, the optimal scheduling period T is unique.*

Proof. The proof can be found in Appendix C. □

Then we try to expand and simplify the objective function $f(T)$ in (20) by exploiting some Markovian properties that it possesses, as direct computation is too complex. We have the following proposition:

Proposition 1 (Objective function expansion)**.** *The objective function* (20) *has the following expansion:*

$$\begin{aligned} J(T) \triangleq & \frac{p}{T^2} \sum_{i=0}^{\infty} (1-p)^i \mathrm{Tr}\left(\sum_{k=iT}^{(i+1)T-1} A^k \bar{P} \left(A'\right)^k \right) \\ & + \frac{p}{T^2} \sum_{i=0}^{\infty} (1-p)^i \\ & \cdot \sum_{k=0}^{T-2} (T-1-k) \mathrm{Tr}\left(A^{iT+k} Q \left(A'\right)^{iT+k} \right) \\ & + \frac{p}{T^2} \sum_{i=1}^{\infty} (1-p)^i (T-1) \sum_{k=0}^{iT-1} \mathrm{Tr}\left(A^k Q \left(A'\right)^k \right). \end{aligned} \tag{21}$$

Proof. The proof can be seen in Appendix D. □

Thus, we could derive the second major contribution of this paper, that is, we obtain the optimal period length as follows:

Theorem 3. *The optimal scheduling period satisfies:*

1) If $\rho(A) = 1$:

$$T = \begin{cases} 1, & \text{if } 0 < p \le \frac{2\mathrm{Tr}(Q)}{2\mathrm{Tr}(\bar{P}) + \mathrm{Tr}(Q)}, \\ \infty, & \text{otherwise}. \end{cases} \tag{22}$$

2) If $\rho(A) < 1$:

$$T = \max\left\{ \left\lfloor \frac{W(\frac{2e^2}{1-p}) - 3}{2\ln(\rho(A))} \right\rfloor + 1, 1 \right\}. \tag{23}$$

3) If $\rho(A) > 1$:

$$T = \min\left\{ \max\left\{ \lfloor \frac{W(\frac{2e^2}{1-p}) - 2}{2\ln(\rho(A))} + 1 \rfloor, 1 \right\}, \lfloor \frac{-\ln(1-p)}{2\ln(\rho(A))} \rfloor + 1 \right\}. \tag{24}$$

where $W(\cdot)$ is the Lambert function.

Proof. The detailed proof can be found in Appendix E. □

Theorem 3 addresses the period length of the optimal scheduling policy for various conditions of the spectral radius, $\rho(A)$.

Remark 2. *By analyzing equations* (22), (23), *and* (24), *it can be seen that at $\rho(A) = 1$, the optimal periodic length is determined by the system error covariance Q and the steady value of the estimate error covariance $\bar{P}$. It is evident that if $\mathrm{Tr}(Q) > 2\mathrm{Tr}(\bar{P})$, then one should always choose continuous data transmission to ensure the freshness and stability of the data, this maintains both timely updates and system stability. When $\rho(A) < 1$, as $\rho(A)$ gets closer to 1, the period approaches 1, despite experiencing packet dropouts in every transmission in a probabilistic context. When the provided spectral radius of the system results in near stability, continuous transmission ensures optimal energy efficiency. When $\rho(A) > 1$, we consider the following special condition: For $p = 1$, the perfect solution that we have identified is also a period equals to 1. This is because the state estimation error covariance grows exponentially over time. In comparison to the linear increase over time, to achieve energy efficiency optimization, it is still preferable to continuously transmit data. Meanwhile, when $\rho(A) > 1$, the system stability boundary imposes an additional constraint $\left\lfloor \frac{-\ln(1-p)}{2\ln(\rho(A))} \right\rfloor$.*

VI. Numerical Simulations

In this section, we illustrate the main results of the paper through the following numerical simulations.

A. Optimal energy efficiency

We set the system parameters as:

$$A = \begin{pmatrix} 0.1 & 0.2 \\ 1.2 & 1 \end{pmatrix} \quad C = \begin{pmatrix} 1 & 2 \end{pmatrix} \quad Q = \begin{pmatrix} 0.3 & 0 \\ 0 & 0.3 \end{pmatrix}$$

and $R = 0.05$. The steady value of the local Kalman filter is calculated as $\bar{P} = \begin{pmatrix} 0.3005 & 0.0029 \\ 0.0029 & 0.4429 \end{pmatrix}$.

We compare the proposed strictly periodic policy under the optimal energy efficiency with the scheduling policy proposed in [12]. As a result, we employ the same parameters detailed in [12] and measure the energy efficiency performance of our calculated optimal scheduling policy compared to that of the aforementioned model.

According to Theorem 3 described previously, the numerically determined period of the optimal scheduling policy is 2. To better demonstrate the effect of simulations, we define the energy efficiency at each time step k as $1/J_k$ and the system performance at each time step k as $1/J_k^e$. Specifically, J_k is given by $\frac{1}{k^2}\sum_{i=0}^{k-1}\mathrm{Tr}(P_i)\sum_{i=0}^{k-1}\theta_i$, and $J_{e,k}$ is $\frac{1}{k}\sum_{i=0}^{k-1}\mathrm{Tr}(P_i)\sum_{i=0}^{k-1}\theta_i$. Fig. 3(a) demonstrates the performance of the optimal policy with $p = 0.7$ compared to other policies such as $\theta_1 = (1,0,1,0,0,1,0,1,0,0,1,0)$ from [12], energy priority transfer policy $\theta_2 = (1,1,1,1,1,0,0,0,0,0,0,0)$ and $\theta_3 = (1,0,1,0,1,0,1,0,0,1,0,0)$ from [11]. For the scenario considered in this paper, our calculations confirm that only the optimal policy θ_p^* yields the best results. Meanwhile, Fig. 3(b) depicts the correlation between our current policy and the system performance. This indicates that since our policy utilizes more energy per unit of time, it yields a substantial improvement in the system performance.

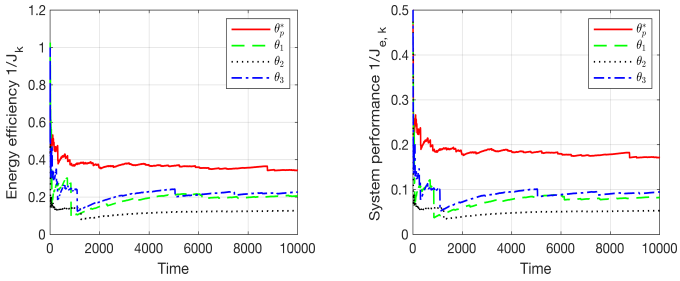

(a) Energy efficiency. (b) System performance.

Fig. 3: Comparison between different policies (when $p = 0.7$).

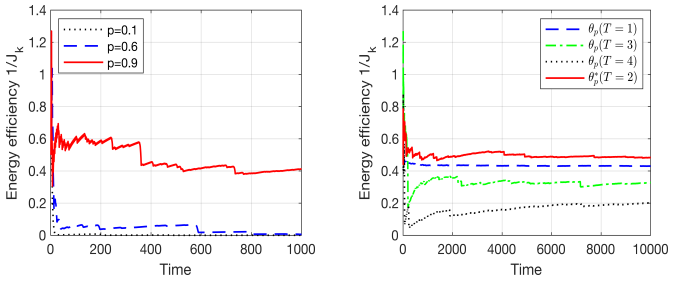

(a) Different arrival probabilities. (b) Different periods.

Fig. 4: Energy efficiency under different parameters.

Then, we employ simulations to verify certain properties of our optimal scheduling policy, such as its convergence. We demonstrate the performance of our proposed optimal policy under different arrival probabilities. With the transmission interval fixed at $T = 2$, it can be observed that when $p = 0.1$, the policy does not satisfy the convergence condition. Fig. 4(a) depicts J_k under different arrival probabilities. It can be observed that when $p = 0.1$, the convergence conditions of Lemma 4 are not satisfied, and J_k exhibits divergence. As the arrival probability increases, the reliability of channel transmission tends to stabilize, leading to improved system performance. Next, we explore the impact of the length of a strict scheduling period on energy efficiency, as shown in Fig. 4(b). The simulation indicates that the system performance gradually improves as the period approaches an optimal value and conversely it decreases as the period deviates from the optimal period. Considering the comparison with policies $\theta_1, \theta_2, \theta_3$, the energy consumption of our proposed optimal energy-efficiency policy is higher than that of the three policies. To ensure fairness, as the optimal policy construction method described in [12], Fig. 6 is plotted given the energy constraints, demonstrating that our proposed policy still guarantees optimal energy ef-

ficiency under different energy constraints. The peak energy efficiency at $6/12$ can be attributed to the balance between the number of transmissions and the resulting system performance. At this ratio, the scheduling period achieves a near-optimal trade-off, where the reduction in energy consumption (fewer transmissions) does not significantly degrade estimation performance. Beyond $6/12$, increasing the transmission count results in diminishing returns for system performance relative to the additional energy expenditure, leading to a decline in energy efficiency.

B. Examples: Extended Simulation Scenarios in Practice

To strengthen the findings, we expand the simulations to include more diverse real-world scenarios, incorporating different sensor types and dynamic communication conditions. We first introduce several common sensor applications. Three representative sensor types are considered: temperature monitoring sensors, inertial measurement units, and air quality sensors. Each sensor's state-space dynamics and noise characteristics are modeled based on real-world specifications. The packet arrival rate of the communication channel is set as 0.7.

- Temperature monitoring sensor in industrial IoT with system dynamics [37]: $x_{k+1} = x_k + w_k$, $y_k = x_k + v_k$ with $Q = 0.01$ and $R = 0.05$;
- Inertial measurement unit (IMU) for position tracking with system dynamics [38]: $x_{k+1} = \begin{bmatrix} 1 & 0.1 \\ 0 & 1 \end{bmatrix} x_k + \begin{bmatrix} 0.005 \\ 0.1 \end{bmatrix} w_k$, $y_k = \begin{bmatrix} 1 & 0 \end{bmatrix} x_k + v_k$ with $Q = \begin{bmatrix} 0.2 & 0 \\ 0 & 0.2 \end{bmatrix}$ and $R = 0.1$.
- Air quality sensor in smart city's application with system dynamics [39]: $x_{k+1} = 0.9x_k + w_k$, $y_k = x_k + v_k$ with $Q = 0.5$ and $R = 1$.

Fig. 5(a) illustrates the performance of the proposed scheduling policy under these diverse scenarios. It demonstrates that in the case of temperature and air quality sensors, which have smaller variations and estimation errors, the energy efficiency is relatively high. Conversely, for sensors like the IMU, which are required to detect pose, the energy efficiency is comparatively low.

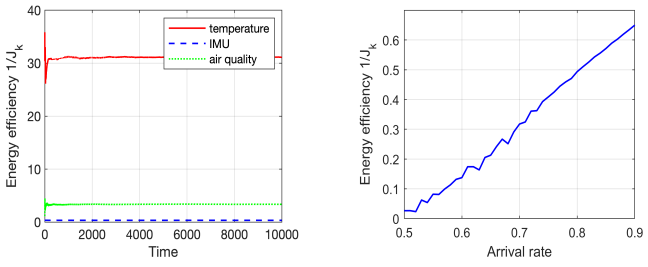

(a) Different sensors. (b) Different probilities.

Fig. 5: Energy efficiency under different practical scenarios.

Then, we evaluate the performance of the proposed scheduling framework under realistic communication environments, we simulate various packet loss scenarios reflecting urban networks, industrial IoT systems, and vehicular communication networks. The packet success arrival probability p is adjusted to reflect the impact of varying packet success arrival probabilities on energy efficiency as follows:

- Urban wireless networks with time-varying success probabilities: typically fluctuating between a maximum transmission success rate of 0.9 and a minimum rate of 0.7.
- Industrial IoT networks with bursty packet loss: normally stable at 0.9, with sudden transitions to a high packet loss probability state of $p = 0.5$.
- Vehicular networks with periodic channel variation: usually represented in a sinusoidal form, for example, $p(k) = 0.7 + 0.2\sin(2\pi k/c_T)$ with channel period c_T.

We find that for practical communication systems, the packet reception rate primarily falls within the range of 0.5 to 0.9. We choose to use the performance characterization at an iteration count of 10,000 as a benchmark, and by employing the dynamic system parameters proposed in Section VI.A, we simulate the mean value of the energy efficiency variation within this range. As can be seen in Fig. 5(b), with the increase of p, the system's energy efficiency improves. This indicates that regardless of the communication channel, as long as the channel quality improves, the energy efficiency will undoubtedly enhance.

C. Monte Carlo Study

The aforementioned simulations demonstrate the variations in optimal energy efficiency from a time-domain perspective. Next, using the Monte Carlo method, we will examine the interrelationships between successful transmission rates, system performance, energy-efficiency ratio, and optimal scheduling period on an average scale.

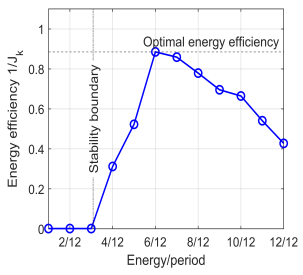

Fig. 6: Comparison of energy efficiency across different energy states.

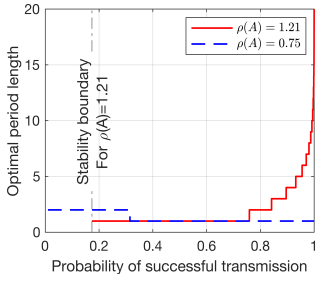

Fig. 7: Correlation between the optimal scheduling period and the probability of successful transmission across varying values of $\rho(A)$.

We analyze how the optimal scheduling period varies with successful packet transmission rates between 0 and 1 for cases where $\rho(A) < 1$ and $\rho(A) > 1$, as shown in Fig. 7. When $\rho(A) < 1$, the optimal scheduling period gradually decreases with increasing probability. In contrast, when $\rho(A) > 1$, it increases.

Moreover, Fig. 8(a) depicts the relationship between the spectral radius of the system matrix, $\rho(A)$, and the optimal scheduling period for a packet transmission rate of $p = 0.7$.

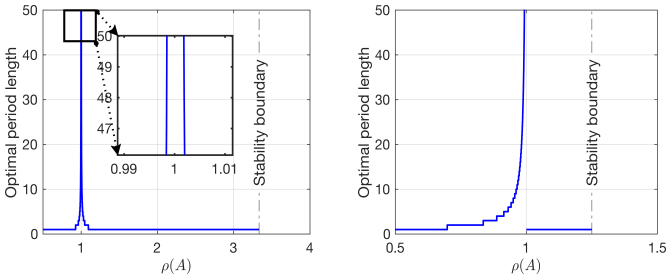

(a) When $p = 0.7$. (b) When $p = 0.2$.

Fig. 8: Evalution of optimal period length T under different $\rho(A)$.

The optimal period length exhibits a monotonically increasing trend when $\rho(A) < 1$ and a monotonically decreasing trend when $\rho(A) > 1$. At first glance, this appears counterintuitive; however, from an energy efficiency perspective, constant transmission can avoid the linear accumulation of system noise in cases of rapid system convergence, while during system divergence it can prevent the exponential accumulation of error covariance.

Furthermore, Fig. 8(b) sketches the graph for a packet transmission rate of $p = 0.2$, where the optimal policy with $\rho(A) = 1$ is not to refrain from sending but to always send off with a period of 1. Besides, we observe that whenever $\rho(A) > 1$ and stability conditions are met, the optimal energy efficiency consistently favors a sending period of 1.

D. Discussions

To enable practical deployment of the proposed periodic scheduling policy, we integrate it into different layers of the communication protocol stack, depending on the system's requirements and constraints. Generally, the proposed scheduling strategy is integrated at the application layer. At this layer, the policy can access system-specific data, such as state estimates and system parameters, making it well-suited for high-level decision-making. It can be embedded in application-layer protocols like Constrained Application Protocol (CoAP) for IoT devices, dynamically adjusting transmission schedules by signaling the medium access control (MAC) layer based on state estimation or other metrics. For example, in a temperature monitoring system, the policy embedded in the CoAP client could calculate the dynamic system parameter and steady error covariance to obtain transmission frequency during stable conditions. At the MAC layer, which controls access to the communication medium, this policy is ideal for implementing real-time scheduling decisions. It can modify transmission schedules directly in the MAC layer queue and interact with energy-efficient protocols like IEEE 802.15.4 (ZigBee). In an industrial IoT system with heterogeneous sensors, for instance, a smart manufacturing setup with sensors monitoring temperature, vibration, and machine health, these sensors have different computational capabilities and energy budgets. We could apply the following integration strategies, such as: in the application layer, the temperature sensors use a CoAP-based application layer to schedule transmissions dynamically, while the vibration sensors utilize MAC-level scheduling in IEEE 802.15.4 to prioritize critical event data during machine faults. Further, the machine health sensors leverage a cross-layer framework combining real-time channel conditions (physical layer) with fault-criticality metrics (application layer) to optimize transmission schedules.

The proposed policy lays a foundation for further improvements on system energy efficiency by co-designing more aspects. For example:

- Cross-layer optimization: Our current approach is that the scheduling decisions $\boldsymbol{\theta}_k$ are based on the trade-off between energy efficiency and estimation accuracy, with the packet success arrival probability p from the physical layer influencing the periodic schedule. We can consider introducing real-time feedback from the MAC and physical layers into the optimization problem. For instance: 1) The success probability p can be dynamically adjusted based on real-time channel conditions (e.g., signal-to-noise ratio (SNR) or interference levels). 2) MAC-layer parameters, such as queue state or contention window size, are incorporated to ensure that scheduling decisions adapt to medium access constraints. Furthermore, the periodic schedule provides a deterministic transmission pattern that simplifies resource allocation at the MAC layer, such as contention window adjustments or slot assignments. At the physical layer, the predictable periodic schedule allows for pre-allocation of resources, such as power or bandwidth, avoiding the need for real-time computations. Thus, the optimization problem would include dynamic variables reflecting channel conditions and MAC-layer feedback, leading to a time-varying periodic schedule. Meanwhile, the conclusions on the derived optimal periodic policy would be extended to include its robustness under dynamic channel conditions and MAC-layer constraints.
- Virtualization technologies: Software-defined networking (SDN) can enable centralized scheduling control, abstracting hardware differences and dynamically allocating network resources. Network function virtualization (NFV) can offload computational tasks from resource-constrained sensors to more capable nodes or cloud infrastructure, thereby improving scalability. In practical applications where real-time computation is required, the adoption of SDN and NFV technologies is beneficial for the implementation and deployment of our scheduling policy. Our current approach is designed for individual sensors without explicit consideration of network-wide coordination or hardware heterogeneity. We can consider implementing the scheduling algorithm within an SDN controller, which would manage and optimize scheduling decisions across a distributed network. The controller could dynamically allocate resources to devices based on their energy levels, computational capacity, and communication needs. Meanwhile, NFV could be employed to virtualize estimation and scheduling functions, enabling lightweight sensors to offload complex computations to more capable nodes or cloud infrastructure. This would

ensure that devices with limited computational capacity can still participate in the scheduling framework effectively. Furthermore, the periodic schedule ensures predictable computational and communication workloads, making it easier to implement scheduling and offloading strategies in NFV frameworks. Edge or cloud resources can be allocated dynamically at predictable intervals, minimizing resource contention. Lightweight devices can offload computations at fixed intervals, simplifying synchronization and reducing latency. Thus, the optimization framework could be extended to consider network-wide resource allocation. Meanwhile, the conclusions on energy efficiency and system robustness would be expanded to include the benefits of centralized scheduling and computation offloading.

- Interplay between communication protocols and control algorithms: We can co-design control algorithms that are resilient to packet delays and losses induced by scheduling. The scheduling framework can prioritize the transmission of data critical to control performance, ensuring stable operation even under constrained communication resources. Meanwhile, the periodic schedule can be dynamically adjusted based on real-time feedback from the control system. For example, if the system's state estimation error exceeds a predefined threshold, then the transmission frequency could be temporarily increased. Our current approach uses the periodic schedule to optimize energy efficiency while maintaining estimation accuracy without explicitly considering control feedback. We can consider introducing control system feedback directly into the scheduling framework. Next, we adjust transmission frequency based on real-time state estimation error or system stability margins. Then, we prioritize data packets critical to control actions, such as those with higher state estimation uncertainty. By ensuring regular state updates, the periodic schedule simplifies the design of control strategies that rely on predictable data availability.

VII. Conclusion

In this study, we have examined the problem of sensor scheduling with a focus on optimal energy efficiency. Advancing prior work that sought to minimize the average estimation error covariance within energy limitations, we have formulated a sensor scheduling approach based on optimal energy efficiency. Our theoretical proofs have confirmed that a periodic scheduling strategy based on optimal energy efficiency invariably results in a strictly periodic pattern, and we have numerically determined the precise scheduling intervals. This research has effectively addressed the challenge of periodic scheduling in single-sensor remote state estimation. Opportunities for future research include extending the current work to coordinated scheduling policies in multi-sensor environments. Furthermore, while this study assumes zero-mean Gaussian noise, full observability, and stabilizability, extending the framework to address more complex scenarios is an important direction for future research. For example, the Kalman filter could be replaced with particle filters or robust H_∞ filtering to handle different noise distributions. Reduced-order observers or subsystem-specific estimation techniques could complement the scheduling framework in scenarios with limited sensor coverage. The scheduling policy could be integrated with robust or predictive control strategies to ensure system performance under instability.

References

[1] Y. Yuan, X. Tang, W. Zhou, W. Pan, X. Li, H.-T. Zhang, H. Ding, and J. Goncalves, "Data driven discovery of cyber physical systems," *Nat. Commun.*, vol. 10, no. 1, pp. 1–9, 2019.

[2] D. I. Shuman, A. Nayyar, A. Mahajan, Y. Goykhman, K. Li, M. Liu, D. Teneketzis, M. Moghaddam, and D. Entekhabi, "Measurement scheduling for soil moisture sensing: From physical models to optimal control," *Proc. IEEE*, vol. 98, no. 11, pp. 1918–1933, 2010.

[3] F. Farokhi and K. H. Johansson, "Stochastic sensor scheduling for networked control systems," *IEEE Trans. Autom. Control*, vol. 59, no. 5, pp. 1147–1162, 2014.

[4] Y. Li, D. E. Quevedo, V. Lau, and L. Shi, "Optimal periodic transmission power schedules for remote estimation of ARMA processes," *IEEE Trans. Signal Process.*, vol. 61, no. 24, pp. 6164–6174, 2013.

[5] G. K. Atia, V. V. Veeravalli, and J. A. Fuemmeler, "Sensor scheduling for energy-efficient target tracking in sensor networks," *IEEE Trans. Signal Process.*, vol. 59, no. 10, pp. 4923–4937, 2011.

[6] S. Han, S. Bian *et al.*, "Energy-efficient 5G for a greener future," *Nat. Electron.*, vol. 3, no. 4, pp. 182–184, 2020.

[7] C. Jiang, Y. Shi, Y. T. Hou, and S. Kompella, "On optimal throughput-energy curve for multi-hop wireless networks," in *Proc. IEEE INFOCOM 2011*. IEEE, 2011, pp. 1341–1349.

[8] Y. Chen, S. Zhang, S. Xu, and G. Y. Li, "Fundamental trade-offs on green wireless networks," *IEEE Commun. Mag.*, vol. 49, no. 6, pp. 30–37, 2011.

[9] D. Jiang, Y. Wang, Z. Lv, W. Wang, and H. Wang, "An energy-efficient networking approach in cloud services for IIoT networks," *IEEE J. Sel. Areas Commun.*, vol. 38, no. 5, pp. 928–941, 2020.

[10] V. Gupta and S. De, "An energy-efficient edge computing framework for decentralized sensing in WSN-assisted IoT," *IEEE Trans. Wireless Commun.*, vol. 20, no. 8, pp. 4811–4827, 2021.

[11] L. Shi, P. Cheng, and J. Chen, "Sensor data scheduling for optimal state estimation with communication energy constraint," *Automatica*, vol. 47, no. 8, pp. 1693–1698, 2011.

[12] Z. Ren, P. Cheng, J. Chen, L. Shi, and Y. Sun, "Optimal periodic sensor schedule for steady-state estimation under average transmission energy constraint," *IEEE Trans. Autom. Control*, vol. 58, no. 12, pp. 3265–3271, 2013.

[13] L. Zhao, W. Zhang, J. Hu, A. Abate, and C. J. Tomlin, "On the optimal solutions of the infinite-horizon linear sensor scheduling problem," *IEEE Trans. Autom. Control*, vol. 59, no. 10, pp. 2825–2830, 2014.

[14] Y. Mo, E. Garone, and B. Sinopoli, "On infinite-horizon sensor scheduling," *Syst. Control Lett.*, vol. 67, pp. 65–70, 2014.

[15] S. Kang, A. Eryilmaz, and C. Joo, "Comparison of decentralized and centralized update paradigms for distributed remote estimation," *IEEE/ACM Trans. Netw.*, vol. 32, no. 2, pp. 1839–1853, 2024.

[16] X. Cao, P. Cheng, J. Chen, and Y. Sun, "An online optimization approach for control and communication codesign in networked cyber-physical systems," *IEEE Trans. Ind. Informat.*, vol. 9, no. 1, pp. 439–450, 2012.

[17] L. Xu, Y. Mo, and L. Xie, "Remote state estimation with stochastic event-triggered sensor schedule and packet drops," *IEEE Trans. Autom. Control*, vol. 65, no. 11, pp. 4981–4988, 2020.

[18] M. Pezzutto, L. Schenato, and S. Dey, "Transmission power allocation for remote estimation with multi-packet reception capabilities," *Automatica*, vol. 140, p. 110257, 2022.

[19] T. Iwaki, J. Wu, Y. Wu, H. Sandberg, and K. H. Johansson, "Multi-hop sensor network scheduling for optimal remote estimation," *Automatica*, vol. 127, p. 109498, 2021.

[20] J. Wei and D. Ye, "On two sensors scheduling for remote state estimation with a shared memory channel in a cyber-physical system environment," *IEEE Trans. Cybern.*, vol. 53, no. 4, pp. 2225–2235, 2021.

[21] W. Xing, X. Zhao, T. Başar, and W. Xia, "Optimal transmission scheduling for remote state estimation in CPSs with energy harvesting two-hop relay networks," *Automatica*, vol. 152, p. 110963, 2023.

[22] M. Nattaf, C. Artigues, and P. Lopez, "A hybrid exact method for a scheduling problem with a continuous resource and energy constraints," *Constraints*, vol. 20, pp. 304–324, 2015.

[23] J. Wei and D. Ye, "Double threshold structure of sensor scheduling policy over a finite-state Markov channel," *IEEE Trans. Cybern.*, vol. 53, no. 11, pp. 7323–7332, 2022.

[24] S. Wu, X. Ren, Q.-S. Jia, K. H. Johansson, and L. Shi, "Learning optimal scheduling policy for remote state estimation under uncertain channel condition," *IEEE Trans. Control Netw. Syst.*, vol. 7, no. 2, pp. 579–591, 2019.

[25] H. Yang, M. Huang, Y. Li, S. Dey, and L. Shi, "Joint power allocation for remote state estimation with SWIPT," *IEEE Trans. Signal Process.*, vol. 70, pp. 1434–1447, 2022.

[26] H.-S. Lee and J.-W. Lee, "Adaptive transmission scheduling in wireless networks for asynchronous federated learning," *IEEE J. Sel. Areas Commun.*, vol. 39, no. 12, pp. 3673–3687, 2021.

[27] H. He, H. Shan, A. Huang, Q. Ye, and W. Zhuang, "Edge-aided computing and transmission scheduling for LTE-U-enabled IoT," *IEEE Trans. Wireless Commun.*, vol. 19, no. 12, pp. 7881–7896, 2020.

[28] A. Zakeri, M. Moltafet, M. Leinonen, and M. Codreanu, "Minimizing the AoI in resource-constrained multi-source relaying systems: Dynamic and learning-based scheduling," *IEEE Trans. Wireless Commun.*, vol. 23, no. 1, pp. 450–466, 2023.

[29] J. P. Hespanha, P. Naghshtabrizi, and Y. Xu, "A survey of recent results in networked control systems," *Proc. IEEE*, vol. 95, no. 1, pp. 138–162, 2007.

[30] G. Welch, G. Bishop *et al.*, "An introduction to the Kalman filter," 1995.

[31] B. D. Anderson and J. B. Moore, *Optimal Filtering*. Courier Corporation, 2012.

[32] Q. Wang, M. Hempstead, and W. Yang, "A realistic power consumption model for wireless sensor network devices," in *Proc. 2006 3rd Annu. IEEE Commun. Soc. Sensor Ad Hoc Commun. Netw.* IEEE, 2006, pp. 286–295.

[33] R. Jurdak, A. G. Ruzzelli, and G. M. O'Hare, "Radio sleep mode optimization in wireless sensor networks," *IEEE Trans. Mobile Comput.*, vol. 9, no. 7, pp. 955–968, 2010.

[34] L. Shi, M. Epstein, and R. M. Murray, "Kalman filtering over a packet-dropping network: A probabilistic perspective," *IEEE Trans. Autom. Control*, vol. 55, no. 3, pp. 594–604, 2010.

[35] M. R. Garey and D. S. Johnson, *Computers and Intractability: A Guide to the Theory of Np-Completeness*. San Francisco, CA: W.H. Freeman & Company, 1979, vol. 174.

[36] B. Sinopoli, L. Schenato, M. Franceschetti, K. Poolla, M. I. Jordan, and S. S. Sastry, "Kalman filtering with intermittent observations," *IEEE Trans. Autom. Control*, vol. 49, no. 9, pp. 1453–1464, 2004.

[37] L. Lyu, C. Chen, S. Zhu, N. Cheng, B. Yang, and X. Guan, "Control performance aware cooperative transmission in multiloop wireless control systems for industrial IoT applications," *IEEE Internet Things J.*, vol. 5, no. 5, pp. 3954–3966, 2018.

[38] Q. Guan, G. Wei, L. Wang, and Y. Song, "A novel feature points tracking algorithm in terms of IMU-aided information fusion," *IEEE Trans. Ind. Inf.*, vol. 17, no. 8, pp. 5304–5313, 2020.

[39] Z. Hu, Z. Bai, Y. Yang, Z. Zheng, K. Bian, and L. Song, "UAV aided aerial-ground IoT for air quality sensing in smart city: Architecture, technologies, and implementation," *IEEE Netw.*, vol. 33, no. 2, pp. 14–22, 2019.

[40] E. Carlen, "Trace inequalities and quantum entropy: An introductory course," *Entropy Quantum*, vol. 529, pp. 73–140, 2010.

APPENDIX A

Proof of Theorem 1: First, we obtain that $J(\boldsymbol{\theta}) = \lim_{N\to\infty} \frac{1}{N}\sum_{k=0}^{N-1} J_r(\boldsymbol{\theta})\mathrm{Tr}(P_k) = \lim_{N\to\infty} \frac{1}{N}\sum_{k=0}^{N-1} \mathrm{Tr}(\mathbb{E}[J_r] P_k)$, where $\mathbb{E}[J_r] \in [0,1]$ is the mathematical expectation that converges to the sequence $\{\theta_k\}$. Further, we introduce the following useful lemma to assist our proof.

Lemma 6 ([14, Theorem 1])**.** *$J(\boldsymbol{\theta})$ is independent of the initial condition Σ but only depends on the scheduling.*

Due to the provision of Lemma 6, we proceed to dilute the demarcations between Σ and $\bar{P}$ within the context, as it is valid for all cases. Our primary concern is to ponder about their existence. We choose a Σ such that $\Sigma > (J(\boldsymbol{\theta}+\varepsilon))I_n$, where $I_n \in \mathbb{R}^{n\times n}$ is the identity matrix. We find that there exists a K, such that for all $N \geq K$,

$$\frac{1}{N}\sum_{k=0}^{N-1} \mathrm{Tr}(\mathbb{E}[J_r]P_k) \leq J(\boldsymbol{\theta}) + \varepsilon. \tag{25}$$

Moreover, there must exist infinitely many scalars k, such that

$$\mathrm{Tr}(\mathbb{E}[J_r]P_k) < J(\boldsymbol{\theta}) + \varepsilon, \tag{26}$$

which implies that

$$\mathbb{E}[J_r]P_k \leq (J(\boldsymbol{\theta}) + \varepsilon)I_n < \Sigma. \tag{27}$$

As a result, we can choose T such that (25), (26) and (27) all hold at the same time, which is also the period T we want to define, i.e., we now define the period schedule $\boldsymbol{\theta}_p$ to be the same as the original schedule $\boldsymbol{\theta}$ from time step 1 to T and repeat itself starting from $T+1$, such that $\theta_{p,kT+j} = \theta_j, \forall k \in \mathbb{N}_0, 1 \leq j \leq T$. And then, we employ mathematical induction to prove $J(\boldsymbol{\theta}_p) \leq J(\boldsymbol{\theta}) + \varepsilon$. For this purpose, we first need to prove the following:

$$P_{kT+j} \leq P_j, \forall k \in \mathbb{N}_0, 1 \leq j \leq T. \tag{28}$$

As P_k is stationary, for each moment J_k, we can consider using expectation $\mathbb{E}[P_k]$ as a substitution and realize the fulfillment of conditions on an overall basis, i.e.,

$$\mathbb{E}[P_k] = \begin{cases} h(\mathbb{E}[P_{k-1}]), & \text{if } \theta_k = 0, \\ pP_k + (1-p)h(\mathbb{E}[P_{k-1}]), & \text{if } \theta_k = 1. \end{cases} \tag{29}$$

Thus, we need to prove:

$$\mathbb{E}[P_{kT+j}](\boldsymbol{\theta}_p) \leq \mathbb{E}[P_j](\boldsymbol{\theta}_p), \forall k \in \mathbb{N}_0, 1 \leq j \leq T. \tag{30}$$

If we assume (30) holds at a certain time $k = k_0$, then we could derive:

$$\mathbb{E}[P_{k_0+T+1}](\boldsymbol{\theta}_p)$$
$$= \begin{cases} h(\mathbb{E}[P_{k_0+T}]) < h(\mathbb{E}[P_{k_0}]) = \mathbb{E}[P_{k_0+1}], & \text{if } \theta_k = 0, \\ pP_{k_0+T+1} + (1-p)h(\mathbb{E}[P_{k_0+T}]) = \mathbb{E}[P_{k_0+1}], & \text{if } \theta_k = 1. \end{cases}$$

According to (27), it is valid at time step $k = 0$, i.e.,

$$\mathbb{E}[P_T](\boldsymbol{\theta}_p) \leq \mathbb{E}[P_0](\boldsymbol{\theta}_p) = \Sigma. \tag{31}$$

which leads to $P_T(\boldsymbol{\theta}_p) \leq P_0(\boldsymbol{\theta}_p) = \Sigma$. We obtain:

$$J(\boldsymbol{\theta}_p) \leq \frac{1}{N}\sum_{k=0}^{N-1} \mathrm{Tr}(J_r P_k(\boldsymbol{\theta}_p)) \leq J(\boldsymbol{\theta}_p) + \varepsilon. \tag{32}$$

Thus, we complete the proof. ∎

APPENDIX B

Proof of Theorem 2: From the construction of $\boldsymbol{\theta}^*$, we just need to prove that for any periodic policy satisfying the condition given in [12, Lemma 2], there always exists a strictly policy with more 0's or less 0's under the energy efficiency constraint.

First, we introduce the following finite sequence definition,

$$\mathrm{seq}_T = 1, \underbrace{0, 0, \cdots}_{T-1 \text{ times}}. \tag{33}$$

And then we define the average estimation error sequence seq_T following the strict period at a certain time T as $\varepsilon_T \triangleq \frac{1}{T}\sum_{k=0}^{T-1}\text{Tr}(P_k)$. We attempt to use mathematical induction to prove that for any two periods $1 \leq T_1 \leq T_2$, it always exists $\varepsilon_{T_1} < \varepsilon_{T_2}$.

Initial Case. We have $\varepsilon_1 = p\bar{P} + (1-p)h(\bar{P})$ and we also have $\varepsilon_2 = ph(\bar{P}) + (1-p)h^2(\bar{P})$, thus it is easy to obtain $\varepsilon_1 < \varepsilon_2$.

Common Case. For any $T > 2$, it can be obtained that

$$\varepsilon_T = ph^{T-1}(\bar{P}) + (1-p)h^T(\bar{P}), \tag{34}$$

thus, it is easily obtained that $\varepsilon_{T+1} - \varepsilon_T > 0$.

According to Lemma 2 and Lemma 3, the optimal periodic policy must consist of two finite sequences, i.e., seq_{t_1} and seq_{t_2}, where the number of '0' of the two sequences differs only by 0 or 1, e.g., '100101001010010...' or '10101010...'. By the way, if the number of '0' differs by 0, then the optimal periodic policy is called a strictly periodic policy.

According to the conclusion in Lemma 3, we need to prove that there is always a better one, based on the energy-efficiency constraint, than Lemma 2, such as a strictly periodic policy with fewer '0' entries or more '0' entries.

For a given optimal scheduling policy $\boldsymbol{\theta}_{t_1,t_2}$ with fixed m and n like Lemma 2, we define its optimal average estimation error as J_e^{opt}, thus its corresponding optimal energy-efficiency objection is defined as $P_{\text{opt}} = \frac{m}{T}J_e^{\text{opt}}$, and then we consider two other strictly periodic scheduling policies, respectively. One is composed of fewer '0' entries from policy $\boldsymbol{\theta}_{t_1,t_2}$, denoted as $\boldsymbol{\theta}_{t_1}$ and the other is composed of more '0' entries, denoted as $\boldsymbol{\theta}_{t_2}$. Further, the number of zeros to be supplemented is α and the number to be reduced is β, respectively. We obtain that $P_m = \frac{m}{T+\alpha}(J_e^{\text{opt}} + \alpha\varepsilon_{t_1})$ and $P_l = \frac{m}{T-\beta}(J_e^{\text{opt}} - \beta\varepsilon_{t_2})$.

It is easy to obtain that,

$$\begin{aligned} P_l - P_{\text{opt}} =& \frac{m}{T-\beta}(J_e^{\text{opt}} - \beta\varepsilon_{t_2}) - \frac{m}{T}J_e^{\text{opt}} \\ =& \frac{m\beta(J_e^{\text{opt}} - T\varepsilon_{t_2})}{(T-\beta)T} < 0 \end{aligned} \tag{35}$$

and

$$P_m - J_e^{\text{opt}} > 0. \tag{36}$$

Since there can only be a difference of one '0', the strict period must be the optimal solution, and it can only be a strict period with one fewer 0's. Thus, we complete the proof. ■

APPENDIX C

Proof of Lemma 5: Since $\boldsymbol{\theta}_{sp}$ depends only on T, we can use $J_e(T)$ to denote $J_e(\boldsymbol{\theta}_{sp})$. According to Lemma 3, the selection range for the optimum is bounded and $J_e(T)$ decreases monotonically. Since T is a discrete variable, we introduce a continuous variable T to perform differentiation for further analysis. While this representation slightly abuses the notation of T, it does not affect the results. We have $J'(T) = \frac{J_e'(T)T - J_e(T)}{T^2}$ and $J''(T) = \frac{J_e''(T)T^3 - 3J_e'(T)T^2 + 2J_e(T)}{T^4}$.

Clearly, by proving the convexity (or concavity) of $J_e(T)$, we can subsequently establish that the optimal solution for $J(T)$ is unique. By the law of large numbers, $J_e(T)$ increases monotonically as p decreases. Therefore, we simplify the problem by considering the case where no packets are lost, i.e., $p = 1$, and other cases are similar to this one. Due to periodic scheduling, we consider the following $J_e(T)$, i.e.,

$$J_e(T) = \frac{1}{T}\sum_{i=0}^{T-1}\text{Tr}\left(A^i\bar{P}(A')^i + \sum_{k=0}^{i-1}A^kQ(A')^k\right). \tag{37}$$

Since a linear transformation applies an affine transformation to the input of a convex function $\text{Tr}(\cdot)$, the convexity is preserved. Thus, we consider (37). Clearly, for any fixed A, $\bar{P}$, and Q, (37) exhibits a linear growth with respect to T. Consequently, $J_e(T)$ is concave. Therefore, the optimal scheduling period T is unique. ■

APPENDIX D

Proof of Proposition 1: We delineate the packet transmission process under uncertain channel conditions utilizing a time-homogeneous Markov chain with recursive properties to characterize the possible states of the packet transmitting and receiving process. Let the state transition be defined by $\tau_{k+1} = f(\tau_k, i, \mu_k)$, with the initial state set to $\tau_0 = 0$. The strict periodicity of the system is established, which forces sensors to initiate data transmission strictly at intervals of T time steps. Consequently, the indicator λ_k, which denotes the action of transmission in the k-th time step, has been substituted with i. Furthermore, since the structure of the Markov chain is invariant with respect to the time index k, we simplify the notation by occasionally omitting the subscript k. The state τ at the subsequent time step transits to a new state τ', following the probability of state transition $\mathcal{P}_{\tau'\tau} = \Pr(\tau'|\tau)$. That is,

$$\begin{aligned} &\Pr(\tau'|\tau, i=1) \\ &= \begin{cases} p & \text{if } \tau' = 0, \\ 1-p & \text{if } \tau' = \tau+1, \\ 0 & \text{otherwise}, \end{cases} \end{aligned} \quad \begin{aligned} &\Pr(\tau'|\tau, i\neq 1) \\ &= \begin{cases} 1 & \text{if } \tau' = \tau+1, \\ 0 & \text{otherwise}. \end{cases} \end{aligned}$$

With this set-up, we derive the subsequent stochastic Markovian dynamical system, $\tau' = f(\tau, T, c')$. Without loss of generality, we assume that the initial state is $\tau = 0$. Owing to the periodic nature of the system, it can be determined that each state is recurrent. Further, we define $f(T)$ based on the Markov property as described above, and the ensuing statement elucidates the central mechanism. Denote by $\pi_{\tau,i}$ as the long-run proportion of time when the Markov chain is in state τ with the definition: $\pi_{\tau,i} = \lim_{N\to\infty}\frac{1}{N}\mathbb{E}\left[\text{num}_{\tau,i}\right]$ and $\sum_{i=1}^{T}\pi_{\tau,i} = \lim_{N\to\infty}\frac{1}{N}\mathbb{E}\left[\text{num}_{\tau}\right]$, where $\text{num}_{\tau,i}$ and num_{τ} means the total number of the pair (τ, i) happening in $(0, N]$ and the total number of τ happening in $(0, N]$, respectively. For the periodic Markov chain, $\pi_{\tau,i}$ is interpreted as the long-run proportion of the time that the Markov chain is in state τ, i.e., $\pi_{\tau,i} = \sum_{\tau}\pi_{\tau,i}\mathcal{P}_{\tau'\tau}$ and $\sum_{\tau}\pi_{\tau,i} = 1$. Thus, we could obtain:

$$\lim_{N\to\infty}\frac{1}{N}\sum_{k=0}^{N-1}h^{\tau_k}(\bar{P}) = \sum_{\tau=0}^{\infty}\left(h^{\tau}(\bar{P}) \times \sum_{i=1}^{T}\pi_{\tau,i}\right), \tag{38}$$

and split $J_e(\boldsymbol{\theta}_p)$ as

$$J_e(\boldsymbol{\theta}_p) = \mathrm{Tr}\left(\left(\boldsymbol{h}^0(\bar{P}), \boldsymbol{h}^1(\bar{P}), \dots\right)\boldsymbol{\pi}\right), \tag{39}$$

where the vector $\boldsymbol{h}^t(\bar{P})$ is denoted by $(\underbrace{h^0(\bar{P}), \cdots, h^0(\bar{P})}_{T \text{ times}})$, and $\boldsymbol{\pi} = (\pi_{0,1}, \dots, \pi_{0,T}, \pi_{1,1}, \dots, \pi_{1,T}, \dots)'$. With definitions similar to the above part, we have the vectors $\boldsymbol{\pi}_{\cdot,i} = (\pi_{0,i}, \pi_{1,i}, \cdots)$ and $\boldsymbol{\pi}_{\tau,\cdot} = (\pi_{\tau,1}, \pi_{\tau,2}, \cdots, \pi_{\tau,N})$, respectively.

For a given periodic policy $\boldsymbol{\theta}_p(z) \in \Theta$, we obtain that in every row vector $\pi_{\tau,\cdot}$, only m entries are non-zero, where the non-zero vector in π is defined as $\hat{\pi}_{\tau,\cdot}$ with their original order. Thus, for the strictly periodic policy $\boldsymbol{\theta}_{sp} \in \Theta$, we have

$$J_e(\boldsymbol{\theta}_{sp}) = \mathrm{Tr}(\boldsymbol{h}\hat{\boldsymbol{\pi}}'). \tag{40}$$

where $\boldsymbol{h} = (\boldsymbol{h}^0(\bar{P}), \boldsymbol{h}^1(\bar{P}) \dots)$ and $\hat{\boldsymbol{\pi}} = (\hat{\pi}_{0,\cdot}, \hat{\pi}_{1,\cdot}, \dots, \hat{\pi}_{T,\cdot}, \dots)$. Thus, the objective function $J(T)$ in (20) can be alternatively expressed as

$$J(T) = \frac{p}{T^2}\sum_{i=0}^{\infty}(1-p)^i \mathrm{Tr}\left(\sum_{j=0}^{T-1} h^{iT+j}(\bar{P})\right), \tag{41}$$

with

$$\begin{aligned} h^T(\bar{P}) =& \underbrace{(A(\dots(A}_{T \text{ times}}\bar{P}A + Q)\dots)A' + Q \\ =& A^T\bar{P}\left(A'\right)^T + \sum_{i=0}^{T-1} A^i Q \left(A'\right)^i. \end{aligned} \tag{42}$$

Therefore, we obtain (21). ∎

APPENDIX E

Proof of Theorem 3: First of all, we simplify $\mathrm{Tr}\left(A^k X (A^k)'\right)$ as:

$$\begin{aligned} \sum_{k=0}^{m(T)} \mathrm{Tr}\left(A^k X (A^k)'\right) \overset{(a)}{\leq}& \sigma \sum_{k=0}^{m(T)} \mathrm{Tr}\left(A^k (A^k)'\right) \\ \leq& \sigma \sum_{k=0}^{m(T)} n\rho^{2k}(A), \end{aligned} \tag{43}$$

where inequality (a) comes from Cauchy-Schwartz inequality, $m(T)$ is a linear function of T, $\{\lambda_i\}, i = 1, 2, \dots, n$ denote the eigenvalues of matrix A, and $\sigma = \mathrm{Tr}(X)$. Further, we denote the trace of $\bar{P}$ and Q as $\sigma_{\bar{p}}$ and σ_q, respectively. The relaxation reformulation of $J(T)$ can be obtained as follows:

$$\begin{aligned} J(T) \leq& \frac{p}{T^2}\sum_{i=0}^{\infty}(1-p)^i\sigma_{\bar{p}} \sum_{k=iT}^{(i+1)T-1} n\rho^{2k}(A) \\ &+ \frac{p}{T^2}\sum_{i=0}^{\infty}(1-p)^i\sigma_q \sum_{k=0}^{T-2}(T-1-k)n\rho^{2(iT+k)}(A) \\ &+ \frac{p}{T^2}\sum_{i=1}^{\infty}(1-p)^i(T-1)\sigma_q \sum_{k=0}^{iT-1} n\rho^{2k}(A). \end{aligned} \tag{44}$$

Clearly, the scaled function is more straightforward. According to [40], the trace function $A \mapsto \mathrm{Tr}[f(A)]$ will keep monotonicity when f is continuously differentiable. Obviously, the following conditions are satisfied, i.e., when k increases, both $\sum_{k=0}^{m(T)} \mathrm{Tr}\left(A^k X (A^k)'\right)$ and $\sigma\sum_{k=0}^{m(T)} n\rho^{2k}(A)$ increase. Thus, given A, n and $m(T)$, the monotonicity of $\sum_{k=0}^{m(T)} \mathrm{Tr}\left(A^k X (A^k)'\right)$ and $\sigma\sum_{k=0}^{m(T)} n\rho^{2k}(A)$ is consistent, thereby revealing that the optimum of $\inf_T\{\text{right-hand side (R.H.S.) of (44)}\}$ is also the optimal solution of Problem 3 over all possible values of T. Then, based on the different properties of the spectral radius $\rho(A)$, we carry out the following proof in three categories.

A. Case $\rho(A) = 1$

We begin by addressing the case when $\rho(A) = 1$. In this case, $J(T)$ becomes

$$\begin{aligned} J(T) =& \frac{n\sigma_{\bar{p}}}{T} + \frac{n(T-1)\sigma_q}{2T} + \frac{n(T-1)(1-p)\sigma_q}{Tp} \\ =& \frac{n(2p\sigma_{\bar{p}} - 2\sigma_q + p\sigma_q)}{2p}\cdot\frac{1}{T} + \frac{n}{2} + \frac{n(1-p)\sigma_q}{p}. \end{aligned} \tag{45}$$

As expressed in equation (45), the monotonicity of the function $J(T)$ is determined by $2p\sigma_{\bar{p}} - 2\sigma_q + p\sigma_q$, i.e., when $\frac{2\sigma_q}{2\sigma_{\bar{p}}+\sigma_q} < p \leq 1$, (45) is monotonically decreasing with respect to T, therefore the optimal scheduling policy is to not transmit. In this case, we need to check the relationship between the lower bound of p and the stability condition (19), i.e., $\mathrm{Tr}(Q) \leq 2\mathrm{Tr}(\bar{P})$. In the other case, when $0 < q \leq \frac{2\sigma_q}{2\sigma_{\bar{p}}+\sigma_q}$, (45) increases monotonically with respect to T. This implies that the optimal period length is always 1.

Next, we move on to the case where $\rho(A) \neq 1$. We discuss the optimal energy-efficiency transmission policy whenever the system is in the convergence range. We will initially examine the scenario where $\rho(A) < 1$. In terms of format, this case is more convenient for calculation.

B. Case $\rho(A) < 1$

To begin with, we reduce equation (44) into a simpler form as shown below:

$$\begin{aligned} &J(T)_{\rho(A)<1} \\ =& \frac{p}{T^2}\sum_{i=0}^{\infty}(1-p)^i \frac{n\sigma_{\bar{p}}\rho^{2iT}(A)\left(1-\rho^{2T}(A)\right)}{1-\rho^2(A)} \\ &+ \frac{p}{T^2}\sum_{i=0}^{\infty}(1-p)^i n\sigma_q\rho^{2iT}(A)\left(\frac{\left(1-\rho^{2(T-1)}(A)\right)}{1-\rho^2(A)}\right. \\ &\left. - \frac{(\rho^2(A) - (T-1)\rho^{2(T-1)}(A) + (T-2)\rho^{2T}(A)}{(1-\rho^2(A))^2}\right) \\ &+ \frac{p}{T^2}\sum_{i=1}^{\infty}(1-p)^i(T-1)\frac{n\sigma_q\left(1-\rho^{2iT}(A)\right)}{1-\rho^2(A)}. \end{aligned} \tag{47}$$

According to Lemma 4, we obtain

$$\rho^{2T}(A)(1-p) < 1 \Leftrightarrow T > \frac{-\ln(1-p)}{2\ln(\rho(A))} \Rightarrow T > 0$$

. In other words, there is no restriction on the selection of T in this case. On this basis, we consider simplifying equation (47)

$$J'(T)=\frac{\text{R.H.S.}+\left(2T(1-\rho^2(A))(1-p)\rho^{2T}(A)+T^2(1-\rho^2(A))(1-p)(2\ln(\rho(A))\rho^{2T}(A)-2T(1-\rho^2(A)))\right)J(T)}{T^2(1-\rho^2(A))-T^2(1-\rho^2(A))(1-p)\rho^{2T}(A)} \tag{46}$$

through the scalar system approach. Then (47) can be further reduced to

$$\begin{aligned}
&J(T)_{\rho(A)<1}\\
=&\frac{pn\sigma_{\bar{p}}(1-\rho^{2T}(A))}{T^2(1-\rho^2(A))}\frac{1}{1-(1-p)\rho^{2T}(A)}\\
&+\frac{pn\sigma_q}{T^2(1-\rho^2(A))}\frac{1-\rho^{2(T-1)}(A)}{1-(1-p)\rho^{2T}(A)}\\
&-\frac{pn\sigma_q}{T^2(1-\rho^2(A))^2}\left(\frac{\rho^2(A)-(T-1)\rho^{2(T-1)}(A)}{1-(1-p)\rho^{2T}(A)}\right.\\
&\left.+\frac{(T-2)\rho^{2T}(A)}{1-(1-p)\rho^{2T}(A)}\right)\\
&+\frac{pn\sigma_q(T-1)}{T^2(1-\rho^2(A))}\left(\frac{1-p}{p}-\frac{(1-p)\rho^{2T}(A)}{1-(1-p)\rho^{2T}(A)}\right)\\
=&\frac{p}{T^2(1-\rho^2(A))(1-(1-p)\rho^{2T}(A))}\left(n\sigma_{\bar{p}}(1-\rho^{2T}(A))\right.\\
&+n\sigma_q(1-\rho^{2(T-1)}(A))-\frac{n\sigma_q}{1-\rho^2(A)}\left(\rho^2(A)-\rho^{2T}(A)\right)\\
&\left.+n\sigma_q(T-1)\rho^{2(T-1)}(A)+b\sigma_q(T-1)(1-p)\rho^{2T}(A)\right)\\
&+\frac{n\sigma_q(1-p)(T-1)}{T^2(1-\rho^2(A))}.
\end{aligned} \tag{48}$$

We set the implicit function $J(T)$ with respect to T and then take the differentials on both sides of the equation (48). Then we obtain the left-hand side (L.H.S.) and the R.H.S. of the equation, respectively, as follows:

$$\begin{aligned}
\text{L.H.S.}=&\left(T^2(1-\rho^2(A))\left(1-(1-p)\rho^{2T}(A)\right)\right)J'(T)\\
&+\left(2T(1-\rho^2(A))\left(1-(1-p)\rho^{2T}(A)\right.\right.\\
&\left.\left.-T(1-p)(2\ln(\rho(A))\rho^{2T}(A))\right)\right)J(T).
\end{aligned} \tag{49}$$

$$\begin{aligned}
\text{R.H.S.}=&2\ln(\rho(A))\rho^{2T}(A)n\\
&\cdot\left(-p\sigma_{\bar{p}}+\frac{\sigma_q p}{1-\rho^2(A)}-\sigma_q(1-p)^2\right)\\
&+2\ln(\rho(A))\rho^{2(T-1)}(A)n\left(-p\sigma_q+\sigma_q(T-1)\right.\\
&\left.+\sigma_q(1-p)(T-1)\right)\\
&+n\sigma_q\rho^{2(T-1)}(A)+n\sigma_q(1-p)\rho^{2T}(A)\\
&+n\sigma_q(1-p).
\end{aligned} \tag{50}$$

As a result, we obtain the derivative (46) of the implicit function.

Here, we have slightly abused the continuous and discrete forms of the function with respect to T, but the existence of the optimal solution ensures that the final result remains unaffected.

We take $J(T)=\frac{1}{T}J_e(T)$ from formula (48) back into the preceding formula, and let $J'(T)=0$ in (46). Due to $J(T)\neq 0$, we obtain

Case. 1:

$$(1-p)\rho^{2T}(A)(1+T\ln(\rho(A)))=1; \tag{51}$$

Case. 2:

$$\text{R.H.S.}=0. \tag{52}$$

Case 1 can be simplified as

$$(1-p)\rho^{2T}(A)(1+T\ln(\rho(A)))=1 \tag{53}$$

$$\Leftrightarrow \ln_{\rho(A)}\left(\rho^{2T}(A)(1+T\ln(\rho(A)))\right)=\ln_{\rho(A)}(\frac{1}{1-p}) \tag{54}$$

$$\Leftrightarrow 2T\ln(\rho(A))+\ln(1+T\ln(\rho(A)))=-\ln(1-p), \tag{55}$$

where $1+T\ln(\rho(A))$ is treated as a whole for computational convenience. The equilibrium point could be solved by the Lambert W function method, i.e.,

$$2(1+T\ln(\rho(A)))+\ln(1+T\ln(\rho(A)))=\ln\frac{e^2}{1-p}, \tag{56}$$

thus $2(1+T\ln(\rho(A)))=W(\frac{2e^2}{1-p})$, yielding the optimal solution for Case 1 as

$$T_{c1}=\frac{W_0(\frac{2e^2}{1-p})-2}{2\ln(\rho(A))}. \tag{57}$$

As the Lambert W function has multiple branches, here we focus on solution W_0 due to $\frac{2e^2}{1-p}>0$.

Based on the proof of Theorem 2 and Lemma 4, we can infer that if the optimal solution exists in two adjacent scheduling periods, then it occurs in the one with the shorter scheduling period.

Next, we consider Case 2. Similar to the calculation method in Case 1, we also use the Lambert W function to obtain a corresponding numerical solution.

We first simplify equation (50) as follows:

$$\begin{aligned}
&2(T-1)\\
&+\ln_{\rho(A)}\left(2\ln(\rho(A))\rho^2(A)\left(-pn\sigma_{\bar{p}}+\frac{n\sigma_q p}{1-\rho^2(A)}\right.\right.\\
&\left.-n\sigma_q(1-p)^2\right)\\
&-2\ln(\rho(A))pn\sigma_q+n\sigma_q+n\sigma_q(1-p)\rho^2(A)\\
&\left.+2\ln(\rho(A))(T-1)\left(n\sigma_q+n\sigma_q(1-p)\right)\right)\\
=&\ln_{\rho(A)}(-n\sigma_q(1-p)).
\end{aligned} \tag{58}$$

For the sake of streamlining the calculation process, we introduce $\mathcal{A}$ to represent $2\ln(\rho(A))\rho^2(A)(-np\sigma_{\bar{p}}+\frac{n\sigma_q p}{1-\rho^2(A)}-n\sigma_q(1-p)^2)-2\ln(\rho(A))pn\sigma_q+n\sigma_q+n\sigma_q(1-p)\rho^2(A)$, $\mathcal{B}$ to represent $n\sigma_q+n\sigma_q(1-p)$, $\mathcal{C}$ to represent $-n\sigma_q(1-p)$ and $\mathcal{X}$ to represent $2ln(\rho(A))(T-1)$, respectively. Consequently,

we derive:

$$\mathcal{X} + \ln(\mathcal{A} + \mathcal{B}\mathcal{X}) = \ln(\mathcal{C}) \tag{59}$$

$$\Leftrightarrow \left(\frac{\mathcal{A}}{\mathcal{B}} + \mathcal{X}\right) + \ln(\mathcal{A} + \mathcal{B}\mathcal{X}) = \ln \mathcal{C} + \frac{\mathcal{A}}{\mathcal{B}} \tag{60}$$

$$\Leftrightarrow e^{\frac{\mathcal{A}}{\mathcal{B}}+\mathcal{X}}(\frac{\mathcal{A}}{\mathcal{B}} + \mathcal{X}) = \frac{1}{\mathcal{B}} e^{\ln \mathcal{C} + \frac{\mathcal{A}}{\mathcal{B}}} \tag{61}$$

$$\Leftrightarrow \mathcal{X} = W\left(\frac{\mathcal{C}e^{\frac{\mathcal{A}}{\mathcal{B}}}}{\mathcal{B}}\right) - \frac{\mathcal{A}}{\mathcal{B}}. \tag{62}$$

Therefore, we conclude that

$$T_{c2} = \frac{W\left(\frac{\mathcal{C}e^{\frac{\mathcal{A}}{\mathcal{B}}}}{\mathcal{B}}\right) - \frac{\mathcal{A}}{\mathcal{B}}}{2\ln(\rho(A))} + 1. \tag{63}$$

To meet the requirements for solving the Lambert W function, we first examine the following range of $W\left(\frac{\mathcal{C}e^{\frac{\mathcal{A}}{\mathcal{B}}}}{\mathcal{B}}\right)$:

$$\frac{\mathcal{C}}{\mathcal{B}} = \frac{p-1}{2-p} > -\frac{1}{2}. \tag{64}$$

It is straightforward to see from the above equation that $\frac{\mathcal{C}}{\mathcal{B}}$ is a monotonically decreasing function with respect to p. Additionally, p is constrained by the convergence condition in Lemma 4. Therefore, the lower bound of $\frac{\mathcal{C}}{\mathcal{B}}$ and its permissible maximum lower bound are as follows:

$$\inf_p \frac{\mathcal{C}}{\mathcal{B}} = \max\left\{-\frac{1}{\rho^{2T}(A)+1}, -\frac{1}{2}\right\}, \tag{65}$$

thus

$$\max \inf_p \frac{\mathcal{C}}{\mathcal{B}} = \max\left\{\left\{-\frac{1}{\rho^2(A)+1}\right\}_{a\geq 1}, -\frac{1}{2}\right\}. \tag{66}$$

and

$$\min \sup_p \frac{\mathcal{C}}{\mathcal{B}} = 0. \tag{67}$$

Owing to the system limitations, we are aware that the system error consistently remains less than the Kalman filter's steady-state error covariance, i.e., $q < \bar{p}$. Thus,

$$\frac{\mathcal{A}}{\mathcal{B}} > \Bigg(2\ln(\rho(A))\rho^2(A)(-p + \frac{p}{1-\rho^2(A)} - (1-p)^2) \\ -2\ln(\rho(A))p + 1 + (1-p)\rho(A)^2\Bigg)/(2-p). \tag{68}$$

With the constraints $0 \leq a < 1$ and $0 \leq p \leq 1$, the observed lower bound and the upper bound of $\frac{\mathcal{A}}{\mathcal{B}}$ are 1 and 2, respectively. According to (66) and (67), the feasible region of $\frac{\mathcal{C}e^{\frac{\mathcal{A}}{\mathcal{B}}}}{\mathcal{B}}$ can only range from $(-1/e, 0)$, in other words, $W\left(\frac{\mathcal{C}e^{\frac{\mathcal{A}}{\mathcal{B}}}}{\mathcal{B}}\right)$ is within the range $(-1, 0)$. Meanwhile, here we focus on solution W_{-1} due to $\frac{\mathcal{C}e^{\frac{\mathcal{A}}{\mathcal{B}}}}{\mathcal{B}} < 0$.

Subsequently, we bring forth the following lemma to illustrate that the zeros of the derivative of $J(T)$ consistently prevail and are restricted to a specific scope.

Lemma 7. *Lambert W_0 function is an increasing bijection and Lambert W_{-1} function is a decreasing bijection.*

To begin with, we are aware that the zero points of $J'(T)$ only need to simultaneously satisfy Case 1 and Case 2, i.e., (51) and (52). Due to the fact that the solution function T_{c1} pertaining to Case 1 increases, while the solution function T_{c2} linked to Case 2 decreases, the T that simultaneously adheres to both Case 1 and Case 2 consistently emerges within their boundary, denoted as $T = (\lfloor T_{c2} \rfloor, \lfloor T_{c1} \rfloor)$. Additionally, as we have already authenticated that the range of $W\left(\frac{\mathcal{C}e^{\frac{\mathcal{A}}{\mathcal{B}}}}{\mathcal{B}}\right)$ amounts to the range $(-1, 0)$, we can deduce that the solution to T is,

$$T = \max\left\{\lfloor \frac{W(\frac{2e^2}{1-p}) - 3}{2\ln(\rho(A))} \rfloor + 1, 1\right\}. \tag{69}$$

The numerical approximation can be obtained through Newton's iteration.

C. Case $\rho(A) > 1$

We come back to equation (44), when $\rho(A) > 1$. We get

$$\begin{aligned} &J(T)_{\rho(A)>1} \\ =&\frac{pn\sigma_{\bar{p}}}{T^2}\sum_{i=0}^{\infty}(1-p)^i \frac{\rho^{2iT}(A)(1-\rho^{2T}(A))}{1-\rho^2(A)} \\ &+ \frac{pn\sigma_q}{T^2}\sum_{i=0}^{\infty}(1-p)^i \Bigg(\frac{\rho^{2(iT+1)}(A)(1-\rho^{2(T-1)}(A))}{(1-\rho^2(A))^2} \\ &+ \frac{(T-1)\rho^{2iT}(A)}{1-\rho^2(A)}\Bigg) \\ &+ \frac{pn\sigma_q(T-1)}{T^2}\sum_{i=1}^{\infty}(1-p)^i \frac{1-\rho^{2T}(A)}{1-\rho^2(A)}. \end{aligned} \tag{70}$$

Based on the boundary conditions of convergence, we can obtain:

$$\rho^{2T}(A)(1-p) < 1 \Leftrightarrow T < \frac{-\ln(1-p)}{2\ln(\rho(A))}.$$

At this point, we must explore the condition $\frac{-\ln(1-p)}{2\ln(\rho(A))} \leq 1$. During this occurrence, as per Lemma 4, the system undergoes divergence. When sending data is essential, the ideal scheduling period remains constant at 1, i.e.,

$$\frac{-\ln(1-p)}{2\ln(\rho(A))} > 1 \Rightarrow (1-p)\rho^2(A) < 1.$$

As a result, the following range is identified:

$$1 < \rho(A) < \sqrt{\frac{1}{1-p}}. \tag{71}$$

According to (71) and the convergence condition, we can easily obtain that (70) is bounded. Therefore, we further simplify it like (48). We can still consider using a similar proof method as above. We first examine the two cases where the derivative equals 0. In Case 1 as (51), we obtain that

$$\ell(\rho(A), T) = (1-p)\rho^{2T}(A)(1 + T\ln(\rho(A))). \tag{72}$$

With regard to $\rho(A)$ and T, the $\ell(\rho(A), T)$ function demonstrates a monotonic growth obviously. As such, we examine the scenario of $T = 1$, and $\rho(A)$ takes on 1 and $\sqrt{\frac{1}{1-p}}$ as

values. We can derive $\ell(1,1) = 1-p$ and $\ell(\sqrt{\frac{1}{1-p}},1) = 1+\ln(\sqrt{\frac{1}{1-p}})$. This validates the feasibility of $\ell(\rho(A),T)=1$ and the resemblance of solution to (57) with $T = \frac{W_0(\frac{2e^2}{1-p})-2}{2\ln(\rho(A))}$.

Then we consider Case 2 like (52), and we just need to check the R.H.S. of (68). Let $\ell(\rho(A))$ = R.H.S. of (68) with respect to $\rho(A)$. We can verify its monotonic behavior by calculating its derivative as

$$\begin{aligned}&\ell'(\rho(A))\\ =&\frac{1}{2-p}\left(2p(\rho(A)+2\rho(A)\ln(\rho(A)))\frac{\rho^2(A)}{1-\rho^2(A)}\right.\\ &+\frac{4p\rho^3(A)\ln(\rho(A))}{(1-\rho^2(A))^2}-(1-p)^2(\rho(A)+2\rho(A)\ln(\rho(A)))\\ &\left.-\frac{2p}{\rho(A)}+2(1-p)\rho(A)\right).\end{aligned} \tag{73}$$

Since $\rho(A) > 1$, the overall $\ell'(\rho(A))$ is monotonically increasing. By substituting the constraint values of $\rho(A)=1$, we can obtain that $\ell'(\rho(A))$ remains greater than 0. In other words, $\ell(\rho(A))$ is monotonically increasing with respect to $\rho(A)$. Then we obtain that the lower bound of $\frac{A}{B} > 1$ is 1, which satisfies the conclusion when $\rho(A) < 1$. Consequently, we can draw a conclusion similar to it, but with the addition of constraint (71), i.e.,

$$T = \min\left\{\max\left\{\lfloor\frac{W(\frac{2e^2}{1-p})-2}{2\ln(\rho(A))}+1\rfloor,1\right\},\lfloor\frac{-\ln(1-p)}{2\ln(\rho(A))}\rfloor+1\right\}. \tag{74}$$

Thus, we complete the proof. ■

Bowen Sun (Member, IEEE) received the B.Sc degree in Automation from Southeast University, Nanjing, China in 2019, where he is currently pursuing the Ph.D. degree in control science and engineering. From 2020 to 2021, he was a guest Ph.D. student at KTH Royal Institute of Technology, Stockholm, Sweden. His research interests include sensor scheduling and stability in CPS.

Xianghui Cao (Senior Member, IEEE) is a professor at Southeast University, Nanjing, China. He received the Ph.D. degree in control science and engineering from Zhejiang University, China, in 2011. He was a Senior Research Associate at Illinois Institute of Technology, Chicago, USA, in 2012-2015. His research interests include cyber–physical systems, wireless network performance analysis, wireless networked control, and network security. He was a recipient of the Best Paper Runner-Up Award from ACM MobiHoc in 2014 and the First Prize of Natural Science Award of Ministry of Education of China in 2017. He also serves as an Associate Editor for IEEE TRANSACTIONS ON INDUSTRIAL INFORMATICS and *ACTA Automatica Sinica*.

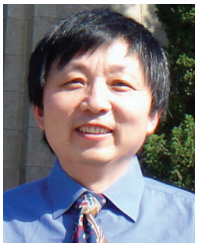

Wei Xing Zheng (Fellow, IEEE) received the B.Sc. degree in Applied Mathematics, the M.Sc. degree in Electrical Engineering and the Ph.D. degree in Electrical Engineering from Southeast University, Nanjing, China, in 1982, 1984, and 1989, respectively. Over the years he has held various faculty/research/visiting positions at Southeast University, Nanjing, China; the Imperial College of Science, Technology and Medicine, London, U.K.; the University of Western Australia, Perth, Australia; the Curtin University of Technology, Perth, Australia; the Munich University of Technology, Munich, Germany; the University of Virginia, Charlottesville, VA, USA; the University of California at Davis, Davis, CA, USA; etc. He is currently a University Distinguished Professor with the Western Sydney University, Sydney, Australia. He has served as an Associate Editor for IEEE TRANSACTIONS ON AUTOMATIC CONTROL, IEEE TRANSACTIONS ON FUZZY SYSTEMS, IEEE TRANSACTIONS ON NEURAL NETWORKS AND LEARNING SYSTEMS, IEEE TRANSACTIONS ON CYBERNETICS, IEEE TRANSACTIONS ON CONTROL OF NETWORK SYSTEMS, IEEE TRANSACTIONS ON CIRCUITS AND SYSTEMS-I: REGULAR PAPERS, and several other flagship journals. He has also served as a Senior Editor for IEEE TRANSACTIONS ON CONTROL OF NETWORK SYSTEMS. He has been an IEEE Distinguished Lecturer of IEEE Control Systems Society. He is a Fellow of IEEE.

Yu Cheng (Fellow, IEEE) received the B.E. and M.E. degrees in electronic engineering from Tsinghua University, Beijing, China, in 1995 and 1998, respectively, and the Ph.D. degree in electrical and computer engineering from the University of Waterloo, Waterloo, ON, Canada, in 2003. He is currently a Full Professor with the Department of Electrical and Computer Engineering, Illinois Institute of Technology, Chicago, IL, USA. His research interests include wireless network performance analysis, information freshness, machine learning, and network security. He was the recipient of the Best Paper Award at QShine 2007 and IEEE ICC 2011, the Runner-Up Best Paper Award at ACM MobiHoc 2014, the National Science Foundation (NSF) CAREER Award in 2011, and the IIT Sigma Xi Research Award in 2013. He has served as several Symposium Co-Chairs for IEEE ICC and IEEE GLOBECOM, and Technical Program Committee (TPC) Co-Chair for IEEE/CIC ICCC2015, ICNC 2015, and WASA 2011. He was a founding Vice Chair of the IEEE ComSoc Technical Subcommittee on Green Communications and Computing. He was an IEEE ComSoc Distinguished Lecturer in 2016-2017. He is an Associate Editor for IEEE TRANSACTIONS ON VEHICULAR TECHNOLOGY, IEEE INTERNET OF THINGS JOURNAL, and *IEEE Wireless Communications*.